Unveiling Stainless-Steel Corrosion in the Drinking Water Distribution System Interdisciplinary Insights on Water Quality and Anticorrosion Design

Pan, Xinyu; Zhao, Yumeng; Dang, Xuhui; Sun, Meng; Liu, Gang; Wen, Gang; Li, Xinlei; Chen, Ao; Jantarakasem, Chotiwat; Pinongcos, Federick

DOI
10.1021/acsestengg.5c00260

Publication date
2025

Document Version
Final published version

Published in
ACS ES and T Engineering

Citation (APA)
Pan, X., Zhao, Y., Dang, X., Sun, M., Liu, G., Wen, G., Li, X., Chen, A., Jantarakasem, C., Pinongcos, F., Li, L., & Ma, J. (2025). Unveiling Stainless-Steel Corrosion in the Drinking Water Distribution System: Interdisciplinary Insights on Water Quality and Anticorrosion Design. *ACS ES and T Engineering*, *5*(6), 1357-1372. https://doi.org/10.1021/acsestengg.5c00260

ACS ES&T Engineering

pubs.acs.org/estengg

Review

Unveiling Stainless-Steel Corrosion in the Drinking Water Distribution System: Interdisciplinary Insights on Water Quality and Anticorrosion Design

Xinyu Pan, Yumeng Zhao,* Xuhui Dang, Meng Sun, Gang Liu,* Gang Wen, Xinlei Li, Ao Chen, Chotiwat Jantarakasem, Federick Pinongcos, Linda Li, and Jun Ma

Cite This: https://doi.org/10.1021/acsestengg.5c00260

Read Online

ABSTRACT: Drinking water distribution system (DWDS) necessitates sustainable, durable, and nonpolluting materials for enhanced water quality of the end-users. Stainless steel (SS) is gaining momentum in DWDS, particularly in end-point distribution facilities such as secondary water storage tanks, pumps, and household water pipes due to its high chemical stability and robust mechanical strength. However, SS's susceptibility to corrosion in given defect areas is of great concern, and there is a lack of fundamental insight on SS corrosion from an interdisciplinary perspective of materials science and environmental science. Herein, the SS corrosion in the DWDS environment is critically assessed, encompassing the basic science of SS corrosion occurrence, its cascading influence on water quality, and anticorrosion strategies. Electrochemical corrosion mechanisms of SS corrosion are specifically differentiated, particularly those initiated at given SS defects, including welding points, grain boundaries, and areas with tensile stress. It is shown that SS corrosion influences water quality by destroying the Cr-rich passive film and releasing Cr, Fe, and other heavy metals from the corrosion scale. The critical factors influencing SS corrosion are subsequently identified, namely, SS elemental composition, SS manufacturing process (e.g., heat-affected zone, stress concentration), and water condition in DWDS (e.g., chlorine, oxygen, sulfate, hydraulic shock, pH). Corresponding strategies are elucidated to facilitate the anticorrosion resistance of SS and improve the water quality, including SS alloying enhancement, SS dispersion strengthening, SS surface treatment/modification, and tuning water condition in DWDS. Overall, this review highlights the importance of controlling SS corrosion, which could provide guidance on the rational design and utilization of SS in DWDS to enhance the ultimate water quality of the end-users and the overall resilience of the DWDS.

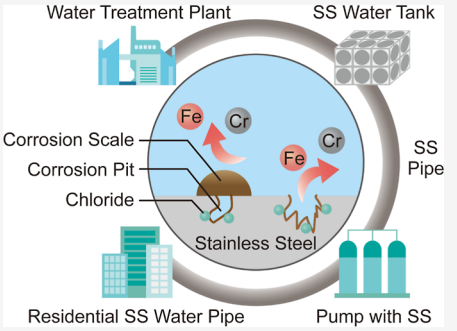

KEYWORDS: *stainless steel, corrosion mechanism, water quality, drinking water distribution system, corrosion prevention*

1. INTRODUCTION

Drinking water distribution is a critical part of the urban water system, determining the ultimate water quality of the end-users.[1] To meet increasingly stringent water quality standards, stainless steel (SS) has been progressively adopted in drinking water distribution system (DWDS) over the past decades due to its high chemical stability, robust mechanical strength, strong pressure resistance, and corrosion-resistant properties.[2,3] In countries such as China, Japan, Germany, and the USA, SS has been widely applied for drinking water distribution in urban water systems.[4,5] Specifically, SS is particularly used in downstream distribution components, including secondary water tanks, pumps, and residential water pipes[6] (Figure 1a).

The selection of appropriate materials is crucial for the effective application of SS in DWDS. SS has been developed into five major categories based on its phases: ferritic SS, austenitic SS, martensitic SS, duplex SS, and precipitation-hardening SS[7−9] (Figure 1b,c). Of these, austenitic SS is most widely used in DWDS due to the properties of high workability, anticorrosion, and relatively low cost.[10,11] These properties can be further enhanced through element doping of Ni, Mn, Mo, etc., resulting in the classification of austenitic SS into Cr−Ni−Mn and Cr−Ni variants[12] (Figure 1d). Among these, Cr−Ni austenitic SS shows better anticorrosion performance, in which 304 and 316 Cr−Ni austenitic SS (see Table S2 for elemental compositions) are most widely used in DWDS.[13]

Although SS exhibits corrosion resistance, it is not completely immune to corrosion. A critical concern with SS is its susceptibility to corrosion at given defect areas, such as crevices and dross on the SS surface. These defects are

Received: March 26, 2025
Revised: May 21, 2025
Accepted: May 22, 2025

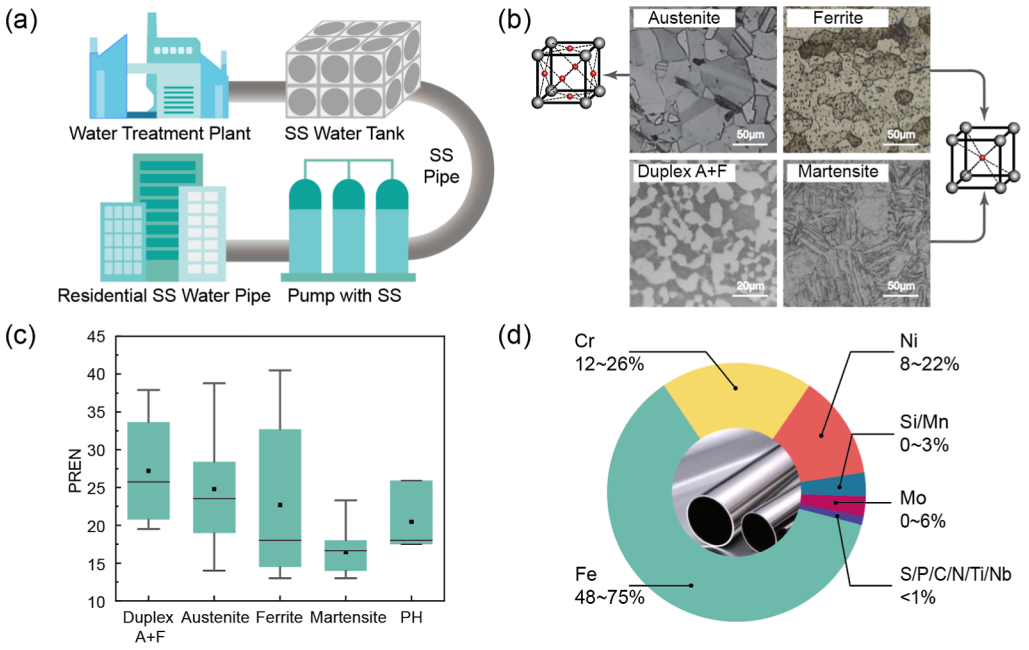

Figure 1. SS in the water distribution system. (a) The diagram illustrates the application scenario of SS in DWDS, including drinking water pipeline, water tank, pump, and residential water pipeline. (b) SEM images of various types of SS.[186−189] Specifically, austenite (A) has a face-centered cubic structure, ferrite (F) and martensite (M) have a body-centered cubic structure, and duplex SS (i.e., duplex A + F) is a combination of austenite and ferrite. The main elements of different types of SS and specific types of SS are listed in Table S1. Reproduced with permission from ref 186, copyright 2014 Elsevier; ref 187, copyright 2012 Elsevier; ref 188, copyright 2002 Elsevier; and ref 189, copyright 2014 Elsevier. (c) Range of pitting resistance value (PREN) of various types of SS, of which the average value of austenitic SS is close to that of duplex SS. The concept of PREN is illustrated in Text S1. (d) Elemental composition range of austenitic SS, which primarily comprises Fe, Cr, and Ni.

typically caused by sequential manufacturing processes of welding and heat treatment, respectively.[14,15] The corrosion in such places can be further intensified by the water environment in DWDS, such as the existence of free chlorine (i.e., HClO, ClO^-, Cl_2), low pH, and frequent hydraulic shock.[16−23] The main forms of SS corrosion in DWDS are pitting corrosion and crevice corrosion,[24,25] while other forms of corrosion including intergranular corrosion and stress corrosion also exist.[26,27] SS corrosion inevitably impacts the quality of the supplied water. A notable example involves the oxidation of Cr(0) from SS into Cr(VI), causing the release of toxic Cr(VI) into the supplied water. Under conditions where free chlorine residuals are maintained at 0.5−1.0 mg L^{-1}, and the residence time reaches 5 days, with all Cr in the corrosion scale present as Cr(0) solids, the concentration of Cr(VI) in tap water can increase to 14 μg L^{-1}, exceeding the California drinking water standard of 10 μg L^{-1}.[28] Other influences include Fe release[29] and other heavy metal (e.g., Al, Mn, Ba, Zn, Cu, Ni, V, Pb) release.[5,30−33]

While the SS corrosion and its water impact have been referred in the past studies, attention has been focused solely on material corrosion or water quality deterioration independently.[34−38] There is a lack of fundamental and systematic insight into SS corrosion in DWDS from an interdisciplinary perspective of materials science and environmental science. Given the above gap, assessing SS corrosion, from the basic science of corrosion occurrence to the cascading influence of corrosion on water quality, along with evaluating corresponding anticorrosion strategies in DWDS, could lay the foundation for the rational and niche design of SS in DWDS, thus improving water quality and system resilience.

In this review, we critically evaluate the basic mechanisms of SS corrosion, analyze its cascading influence on DWDS water quality, and further propose the SS corrosion control techniques. Focusing on the intrinsic property of SS, we first analyze the essential cause of corrosion and corrosion scale from a microscopic level, during which the physicochemical transformations are also discussed. Then based on the SS corrosion phenomena, the impact of corrosion on water quality is assessed. From a material perspective, we underscore that the main forms affecting water quality are the release of Cr, Fe, and other heavy metals from the SS scale. Further, we evaluate the influencing factors on SS corrosion and water quality, emphasizing material, manufacturing process, and water environment aspects. Finally, based on the analysis of these influencing factors, a comprehensive strategy for corrosion control and water quality control is proposed.

2. CORROSION MECHANISMS OF SS IN DWDS

2.1. SS Corrosion Mechanisms. To explore the impact of SS corrosion on water quality in DWDS, it is essential to understand the fundamental mechanism of SS corrosion from a perspective of materials science. For SS, the Cr content is generally higher than 12 wt %, which forms a passive film on the SS surface.[39] This chromium-enriched film is thin (<5 nm),[40] continuous, pore-free, hardly soluble, and self-repairing (i.e., forming a new passive film for surface protection after damage).[41] The passive film on SS acts as a protective barrier, offering anticorrosion properties and extending its lifespan in DWDS. However, corrosion may still occur under specific conditions within the DWDS. Because of the existence of free chlorine in drinking water and given defects in SS introduced during the manufacturing process, the SS is primarily weakened by electrochemical corrosion. Arising from electrochemical reactions, the corrosion scenarios of SS in DWDS include pitting corrosion, crevice corrosion, intergranular

https://doi.org/10.1021/acsestengg.5c00260
ACS EST Engg. XXXX, XXX, XXX−XXX

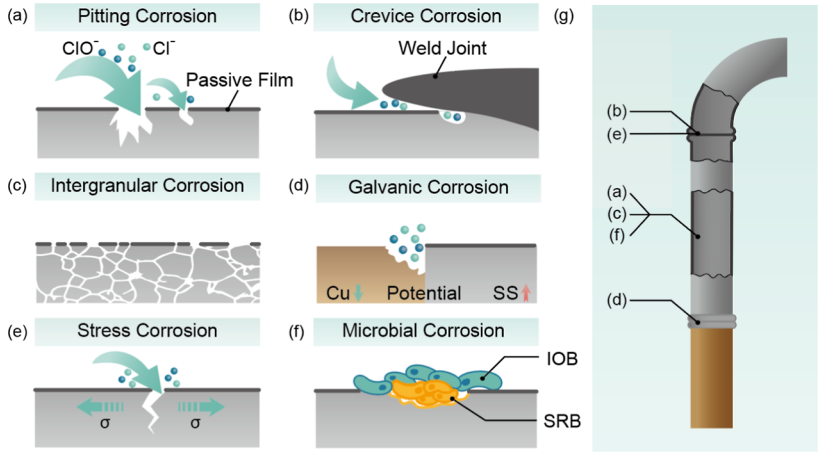

Figure 2. Corrosion scenarios of SS. (a) Pitting corrosion, in which chloride destroys the passive film and leads to corrosion. (b) Crevice corrosion, in which the gap between weld and SS is susceptible to corrosion in the presence of chloride. (c) Intergranular corrosion, which regularly occurs in SS with high carbon content (>0.03 wt %). (d) Galvanic corrosion, occurring in the presence of chloride when different metals are joined (e.g., copper and SS). (e) Stress corrosion, which occurs in the presence of chloride under applied stress caused by the manufacturing process. (f) Microbial influenced corrosion, where iron-oxidizing bacteria (IOB) consumes oxygen in the medium, establishes a favorable growth environment for anaerobic sulfate-reducing bacteria (SRB), and subsequently facilitates SS corrosion by SRB. (g) Diagram illustrating possible corrosion sites of scenarios (a–f) in a piece of the SS pipe.

corrosion, stress corrosion, and galvanic corrosion, with pitting and crevice corrosion being the predominant forms.[24−27] In the above scenarios, corrosion initiating points act as small anodes, while the surrounding uncorroded areas act as large cathodes, thereby accelerating electrochemical corrosion. Additionally, SS is susceptible to microbiological influenced corrosion,[42] which will also be addressed.

2.1.1. Pitting Corrosion and Crevice Corrosion. Pitting corrosion and crevice corrosion are the most common forms of SS corrosion in DWDS.[43−45] The chloride concentration in DWDS is low (<2 mg L^{-1}), but corrosion can still occur over time. Evident pitting corrosion has already been observed in a secondary water supply tank after two years of service.[46] Although the initiation mechanisms differ between these two corrosion scenarios, their propagation mechanisms share similarities. In terms of initiation mechanisms, for pitting corrosion, the attack of chloride ions in DWDS breaks the passive film of SS[47] and leads to the emergence of Fe(0) and Cr(0) as microanode regions, which are surrounded by the passive film as cathodic regions. In chloride containing water, SS gradually dissolves at these microanode regions, generating pits at the corrosion initial points on the SS surface[47] (Figure 2a). For crevice corrosion, there are inherent structural defects for initiating corrosion (Figure 2b), which frequently occur in the welding locations, corrosion scales, and sludge deposits of SS pipes and tanks.[16,43] Further, the propagation of SS corrosion in DWDS can be intensified by an increase in the chloride ion concentration, pH decrease, and reduced oxygen levels within pits and crevices.[48,49] After corrosion occurs, Cr and Fe from SS will diffuse into water, thus impacting the water quality.

2.1.2. Intergranular Corrosion. SS is prone to corrode at locations with manufacturing defects, in which intergranular corrosion is a typical scenario. Intergranular corrosion in SS occurs along or near grain boundaries and leads to the disintegration of the SS surface (Figure 2c), causing metal particles to detach and enter water by the impact of hydraulic flow.[50] The corrosion is typically found in thermally sensitive SS (i.e., the material's composition is significantly affected by temperature changes) that has been subjected to thermal processing during material manufacturing and welding without adequate heat treatment.[51] The manufacturing defects are formed after exposure to sensitization temperature of 450−850 °C[52−54] during which carbon rapidly diffuses toward grain boundaries in SS. Subsequently, carbon reacts with chromium, leading to the formation of chromium-rich phases like Cr_7C_3 and $Cr_{23}C_6$ in the grain boundaries of SS.[55,56] Due to chromium's slow diffusion rate and its inability to replenish promptly from the interior part of the grains, chromium-depleted regions tend to form along the grain boundaries. When the weight percentage of chromium drops below 11%, the chromium-depleted regions along the grain boundaries become anodic sites, while the grains act as cathodic sites.[50] Such SS configuration in DWDS forms a large cathode and small anode structure, triggering rapid corrosion along the grain boundaries and forming a surface that is easy to be peeled off (Figure S1).

2.1.3. Galvanic Corrosion. In DWDS, scenarios like pipe replacement often lead to the junction of different pipe materials with different potentials. Under this circumstance, galvanic corrosion may occur (Figure 2d). As the corrosion resistance of SS is higher than those of most pipe materials, galvanic corrosion generally occurs on other metals connected to SS. For instance, copper- and lead-base pipes can be corroded when connecting to SS pipe due to their lower corrosion potentials. Subsequently, such corrosion may accelerate the release of copper or lead into DWDS.[57−59] Under the SS-Cu-Pb pipe connection method, galvanic corrosion can induce fluent electron transport [SS ← e^-(Cu) ← e^-(Pb)], resulting in the Pb release of 652 μg L^{-1} after a 90 day experiment with tap water (systems is kept stagnant for 1 d and replenish with fresh tap water every day), which significantly exceeds the standards for drinking water quality in China (10 μg L^{-1}).[60] The connection of SS with other carbon steels like SA508[61] or 1020 carbon steels[62] (see Table S2 for elemental compositions) may also lead to the corrosion of the latter. SA508 and 1020 carbon steels do not contain chromium, resulting in a lower corrosion potential and

https://doi.org/10.1021/acsestengg.5c00260
ACS EST Engg. XXXX, XXX, XXX−XXX

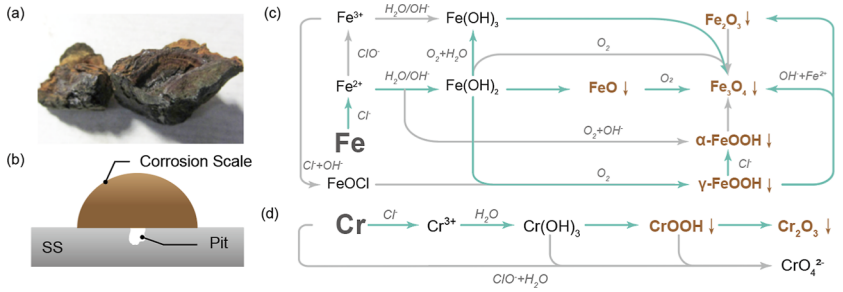

Figure 3. Morphology and generation mechanism of corrosion scale formed on SS. (a) Morphology of the corrosion scale.[5] Reproduced with permission from ref 5. Copyright 2016 Elsevier. (b) Schematic diagram of the SS corrosion scale formation mechanism. The corrosion scale is generally formed on pitting sites. (c,d) Transformation processes related to Fe and Cr during the formation of the SS corrosion scale. Green arrows depict primary reaction processes, gray arrows indicate secondary reaction processes, and brown compounds represent components of the corrosion scale (Table S3).[71−82]

a higher susceptibility to corrosion. Moreover, if the microstructure of solder for welding is changed after hot processing (e.g., from austenite to martensite), its corrosion potential will decrease.[63,64] When the solder acts as an anode and the rest of the SS acts as a cathode, the SS will have a tendency to corrode and lead to rust, leakage, and water pollution (Figure S2).

2.1.4. Stress Corrosion. Stress corrosion occurs under the synergistic effects of tensile stress and corrosive media (Figure 2e). In the case of SS pipe, tensile stress can originate from the fabrication and installation processes such as welding, hot or cold working, and external loads. Further, the risk of stress corrosion gradually increases with the rising concentration of halide ions in DWDS.[65] For instance, the heat-affected zones (the region where the base metal remains in the solid state but undergoes significant microstructural and property changes due to the welding thermal cycle) formed by welding in 304 SS and 316 SS have undergone stress-corrosion-induced cracking in the presence of chloride ions in DWDS.[66,67] After corrosion occurs, cracks propagate perpendicularly to the direction of tensile stress, expanding through transgranular, intergranular, or mixed modes.[68] Although the corrosion products resulting from stress corrosion are limited, they are often difficult to observe with the naked eye and can lead to the rupture of water pipes, making it a hazardous form of pipeline failure.

2.1.5. Microbiologically Influenced Corrosion. Microorganisms present in SS pipelines and tanks can actively contribute to corrosion and exhibit detrimental impacts on the water quality (Figure 2f). Microbiologically influenced corrosion is directly triggered by the life activities of microorganisms or by the substances produced through their metabolic processes. The microorganisms reported to induce SS corrosion are primarily through the synergistic interactions of SRB and IOB. In this process, SRB and IOB collaborate to form a biofilm on the metal surface. The biofilm typically consists of extracellular polymeric substances and corrosion products produced by SRB and IOB.[69,70] IOB consumes oxygen in the medium, creating a suitable anaerobic environment for the SRB. SRB will then use elemental iron as the electron donor to produce energy for maintenance, subsequently leading to corrosion of SS.

2.2. SS Corrosion Scale. As the corrosion process progresses and corrosion products gradually form, corrosion scales can develop on the surface of corroded SS pipes and tanks. In the operation of DWDS, corrosion scales have been observed in valves and pipes.[5,71] In terms of the structure of SS corrosion scale, the typical morphology is the multilayer hemispherical pod-shape[5] (Figure 3a). Such SS corrosion scale generally develops on corrosion pits (Figure 3b), where metal hydroxides continuously migrate from the pit to the SS surface. Under hydraulic forces in DWDS, corrosion products accumulate and adhere to the SS passive film.[30,31] Eventually, as the size of the corrosion pit gradually grows, the amount of dissolved metal increases, leading to a further expansion of the corrosion scale. In addition, microscopic crack structures can be seen in the SS corrosion scale (Figure S3), and the cracks are likely to accumulate and release heavy metals into DWDS.

In terms of chemical components of the SS corrosion scale, the primary elements of the corrosion scale are Fe and Cr, including FeO, α-FeOOH, γ-FeOOH, Fe_2O_3, Fe_3O_4, CrOOH, and Cr_2O_3.[71−73] Their generation pathways are shown in Figure 3c,d (for the specific chemical equations, see Table S3). Fe and Cr in SS undergo anodic metal dissolution reactions with chloride ions in water, forming Fe^{2+} and Cr^{3+}.[74,75] The formation of Fe^{2+} and Cr^{3+} then induces continuous migration of chloride ions into the pit to maintain electrical neutrality and thus accelerates the reaction progress. Because of the presence of free chlorine in DWDS, Fe^{2+} is partly oxidized into Fe^{3+}.[76] Further, Fe^{2+}, Fe^{3+}, and Cr^{3+} ions undergo hydrogenation, which leads to the formation of metal hydroxides, i.e., $Fe(OH)_2$, $Fe(OH)_3$, and $Cr(OH)_3$.[77] For $Fe(OH)_2$, part of $Fe(OH)_2$ transforms into $Fe(OH)_3$ in the presence of dissolved oxygen and further transforms into Fe_3O_4,[78,79] while the other part dehydrates and forms FeO and FeOOH.[76] Additionally, FeO can also be oxidized into Fe_3O_4 under the influence of dissolved oxygen.[74,75] The other hydroxides including $Fe(OH)_2$ and $Cr(OH)_3$ change into FeOOH and CrOOH, respectively, by dehydration.[77] FeOOH typically exists as γ-FeOOH and α-FeOOH in the SS corrosion scale. Specifically, γ-FeOOH is formed in the early stage of corrosion, then transforms into α-FeOOH as the oxidation time increases.[80] As the reaction time prolongs, FeOOH and CrOOH continue dehydrating and generate Fe_2O_3 and Cr_2O_3.[81] Notably, the continuous buildup of corrosion products can hinder the diffusion of dissolved oxygen within the scale. In situations where dissolved oxygen is less than 0.5 mg L^{-1} or the corrosion potential is over 300 mV (SHE), FeOOH can transform to Fe_3O_4.[76,79,82,83] The above analysis demonstrates that within corrosion scales, coprecipitation occurs among FeO, α-FeOOH, γ-FeOOH, Fe_2O_3, Fe_3O_4, CrOOH, and Cr_2O_3, constituting major components of the corrosion products. Such components of the SS corrosion scale could act as a source of metal ions, diffusing metal ions into water and deteriorating water quality.

https://doi.org/10.1021/acsestengg.5c00260
ACS EST Engg. XXXX, XXX, XXX−XXX

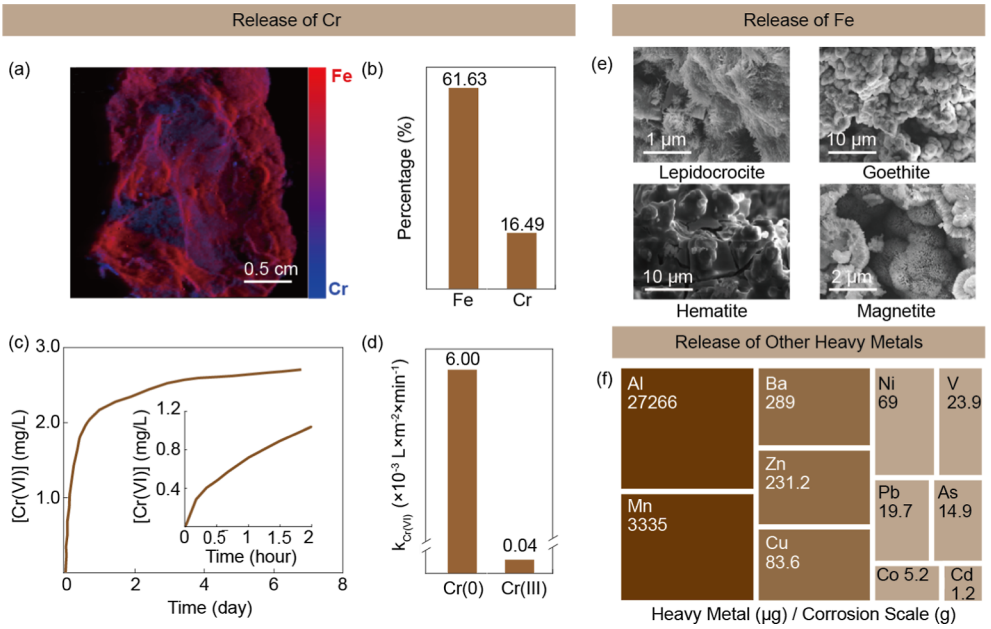

Figure 4. Impact of SS corrosion on water quality, mainly evidenced by Cr, Fe, and other heavy metal release. (a) Element distribution on the SS corrosion scale.[5,28] Reproduced from ref 28. Copyright 2020 American Chemical Society. (b) Weight percentage of main metal elements in the SS corrosion scale, with Cr accounting for approximately 16 wt %.[5,28] (c) Release of Cr(VI), enabled by HOCl oxidation, from the SS corrosion scale as a function of time.[28] (d) Reaction rate constants for the conversion of Cr(0) and Cr(III) to Cr(VI), indicating that the conversion from Cr(0) to Cr(VI) is the primary pathway of Cr(VI) release.[28] (e) SEM image displaying the Fe oxide on the SS corrosion scale.[5,86] Reproduced with permission from ref 5. Copyright 2016 Elsevier. (f) Presence of average weight of heavy metals within the corrosion scale, where larger area sizes represent higher orders of magnitude in heavy metal concentrations in the corrosion scale.[87,88] The detailed experimental data can be found in Table S4.

3. IMPACT OF SS CORROSION ON WATER QUALITY

3.1. Release of Cr and Fe. The release of Cr caused by SS corrosion constitutes a potential threat to the water quality. Cr(VI) exposure may lead to lung cancer, liver damage, and reproductive impairment. Considering its acute toxicity and carcinogenic properties, the U.S. EPA designates Cr(VI) as a high-priority contaminant.[28] Cr is found in the SS corrosion scale, and it exhibits a content similar to that of Cr in the SS itself, typically surpassing 12 wt %[5,28] (Figure 4a,b). In the SS corrosion scale, Cr presents as spherical single crystals formed by direct homogeneous deposition.[71] Regarding the chemical states of Cr in the SS corrosion scale, Cr exists in the forms of Cr(0), Cr_2O_3, and CrOOH. In the presence of free chlorine, species of Cr(0), Cr_2O_3, and CrOOH can be further oxidized to Cr(VI) (i.e., chromate CrO_4^{2-}) and release into DWDS[5,28,84] (Figure 3d)

$$Cr_{0(s)} + 3HOCl + H_2O \rightarrow CrO_4^{2-} + 5H^+ + 3Cl^- \quad (1)$$

$$2Cr_{(III)(s)} + 3HOCl + 5H_2O \rightarrow 2CrO_4^{2} + 13H^+ + 3Cl^- \quad (2)$$

The release of Cr(VI) exhibits an initial rapid increase followed by a subsequent leveling off with prolonged reaction time in the HOCl solution (chlorine-based disinfectants, such as NaClO and chloramines, commonly exert their disinfecting effect by hydrolyzing to form HOCl) (Figure 4c). Throughout the reaction, while Cr(III) oxides can transform into Cr(VI), Cr(0) is the determining factor for the release of Cr(VI) in DWDS. Compared with Cr(III), the accelerated reaction between HClO and Cr(0) results in a more rapid release of Cr(VI) from SS (Figure 4d). This phenomenon occurs when HClO reacts with Cr(0) within SS after the destruction of the Cr(III)-rich passive film on the SS surface.[28]

The release of Fe from SS is also a potential factor that influences water quality. Although Fe does not possess toxicity like Cr, the release of Fe can lead to the occurrence of red water issue and impart a metallic taste, affecting the aesthetic properties of water.[85] The beginning of corrosion pits in SS in a chloride-containing solution is attributed to the anodic dissolution of iron from the SS surface.[29] During the oxidation process, FeO, $Fe(OH)_2$, $Fe(OH)_3$, α-FeOOH, γ-FeOOH, Fe_2O_3, and Fe_3O_4 can be formed (Table S2), and present as crystalline structures like lepidocrocite, goethite, hematite, and magnetite[5,86] (Figure 4e). Due to the weak bonding strength of these crystalline structures with the SS surface, the oxidation products of Fe will ultimately enter water and affect water quality as the hydraulic conditions fluctuate in SS tanks or pipelines.[71]

3.2. Release of Other Heavy Metals and Pipe Leakage. The SS corrosion scale is susceptible to accumulating other heavy metals (e.g., Al, Mn, Ba, Zn, Cu, Ni, V, and Pb) from DWDS and releasing them into water, attributed to the similar characteristics shared with the cast iron corrosion scale. To investigate the mechanism of aggregation of heavy metals, it is necessary to analyze the structure of the corrosion scale. Similar with cast iron corrosion, the SS corrosion scale is formed primarily by electrochemical corrosion with Fe[5,80] and exhibits loose and porous crystalline microstructures showing a high propensity to adsorb heavy metals from water (Figure 4e).[87] While there is no reported literature regarding the adsorption of heavy metals by SS corrosion scales, the adsorption situation of cast iron corrosion scale can be used to infer the elemental adsorption tendencies of the SS

https://doi.org/10.1021/acsestengg.5c00260
ACS EST Engg. XXXX, XXX, XXX−XXX

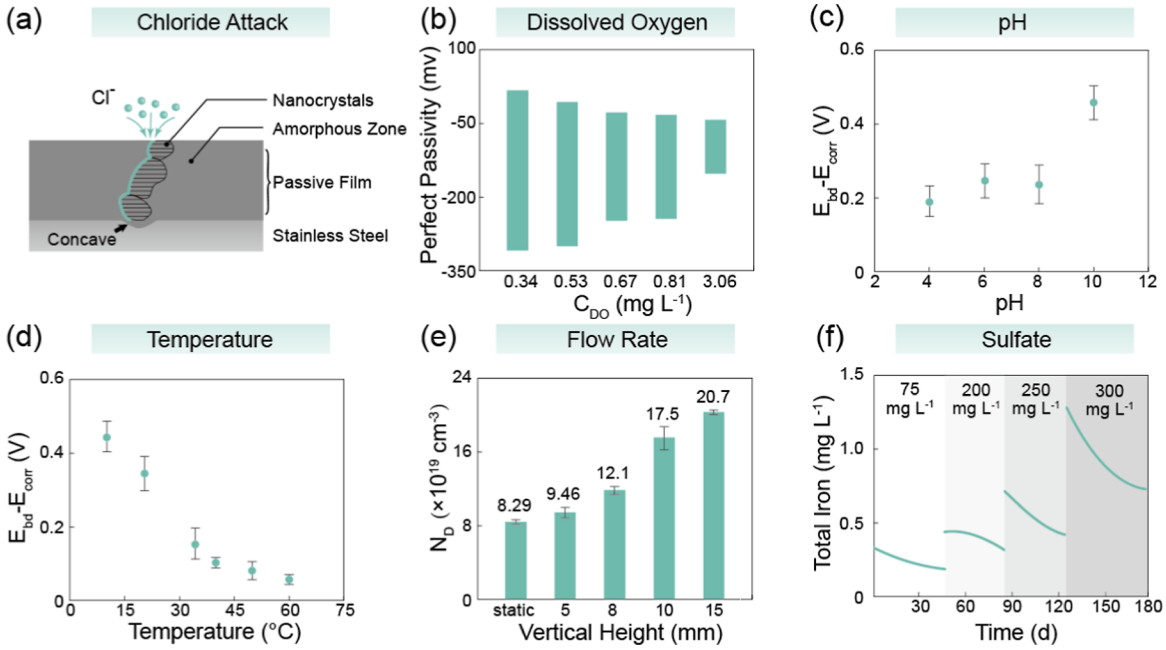

Figure 5. Key factors impacting SS corrosion in DWDS. (a) Corrosion of SS by chlorine attack. The diagram illustrates that the chloride ion corrodes the SS surface through the channel between nanocrystals and the amorphous zone generated in the passive film. The detailed figure is placed in Figure S4. (b) Influence of dissolved oxygen on the SS corrosion. As dissolved oxygen concentration rises, the perfect passivity range gradually diminishes, increasing the probability of corrosion.[100−102] The exact value can be found in Figure S5. (c) Impact of the pH on SS corrosion. Pitting corrosion occurs when the free corrosion potential (E_{corr}) surpasses the passivity breakdown potential (E_{bd}). Higher pH leads to larger difference between E_{corr} and E_{bd}, further lowering the tendency for pitting corrosion.[49,107] (d) Influence of temperature on SS corrosion, where the increase of temperature causes the decrease of $E_{bd}-E_{corr}$ and subsequent higher corrosion tendency.[49] (e) Influence of water flow by 6 h on SS corrosion. The *x*-axis represents the vertical height between the water source and SS, which indicates the water flow rate. The *y*-axis denotes donor density (N_D), representing the vacancies in the SS passive film, which is calculated from Mott−Schottky analysis. Increased water flow rate causes higher N_D and thus higher corrosion tendency.[118] (f) Influence of sulfate concentration (mg L^{-1}) on corrosion scale within a time range of 180 days. As the sulfate concentration increases, the total iron concentration in the solution rises, thereby intensifying water contamination.[123] The original figure is placed in Figure S6.

corrosion scale. Al and Mn are the most abundantly adsorbed metals besides Fe in the corrosion scale, attributed to the influence of groundwater in the pipeline. In addition, trace amounts of heavy metals such as Ba, Zn, Cu, Ni, Pb, V, As, Co, and Cd are also detected (Figure 4f indicates the weight percentages of heavy metals in the corrosion scale).[87,88] Given the porous and loose microstructure, SS corrosion scales are not firmly attached to the pipe or tank and can be easily removed.[71] In addition, the release of heavy metals from the corrosion scale is easily influenced by the water condition.[34] During the operation of DWDS, with factors such as water flow scouring, fluctuations in pipeline pressure, or changes in water source,[89] the corrosion scale and the contained heavy metals will diffuse into water, leading to red water and heavy metal release.

Induced by SS corrosion, leakage in SS facilities is also a potential source of water quality pollution in DWDS.[90] The presence of water pressure and external forces (e.g., earth pressure, residual stress) in DWDS can intensify stress corrosion on the SS surface, resulting in heightened risk of pipe cracking.[91] After cracking, the pipeline is no longer a closed system and will directly contact with soil. Pump operation, pipe replacement, or valve closure/opening can induce negative pressure, allowing soil particles, bacteria, viruses, and other pollutants from the surrounding environment to enter the cracking point, leading to water contamination in DWDS.

4. CRITICAL FACTORS INFLUENCING SS CORROSION

4.1. SS Elemental Composition. The properties of SS materials fundamentally determine their corrosion resistance in DWDS. The impact of materials on SS corrosion is primarily reflected in the elemental composition of SS. Carbon (C) is the most prevalent corrosion-inducing element in SS and has a crucial role in intergranular corrosion. When SS is exposed to high-temperature sensitization (450−850 °C) during SS fabrication and SS pipe installation by welding, Cr_7C_3 and $Cr_{23}C_6$ can form in SS. The content of Cr_7C_3 and $Cr_{23}C_6$ tends to increase as exposure time prolongs, contributing to the risk of the aforementioned intergranular corrosion. Therefore, controlling the content of C can be an effective way to mitigate intergranular corrosion. When the content of C is less than 0.02 wt %, the tendency for intergranular corrosion can be mitigated.[92,93] Sulfur (S) and manganese (Mn) are additional elements that necessitate reduction in SS as they show a propensity to form MnS during the steel smelting process. MnS is susceptible to acidic chloride solution and often serves as a corrosion source, diminishing SS resistance to pitting corrosion and crevice corrosion.[94] Generally, the maximum contents of Mn and S in austenitic SS should be below 2 and 0.03 wt %.[95]

4.2. SS Manufacturing Process. The manufacturing process of SS can affect its material properties, thereby influencing its corrosion resistance in DWDS. The manufacturing of SS materials and buried installation processes of SS pipes mostly involve the thermal processing of SS, which is

https://doi.org/10.1021/acsestengg.5c00260
ACS EST Engg. XXXX, XXX, XXX−XXX

commonly implemented through SS welding. During welding, SS undergoes short-term thermal cycles (rapidly heated and reverted to the initial state), forming a heat-affected zone adjacent to the welding position of SS. Short-term thermal cycles can lead to the precipitation of chromium-rich phases and detrimental intermetallic compounds (i.e., σ-phase and χ-phase. For specific information, see Table S5). This, in turn, causes chromium depletion in weld and heat-affected zones in SS and decreases corrosion resistance.[96] Additionally, chromium-rich phases can induce uneven microstructures at grain boundaries in heat-affected zones. Electrochemical analysis indicates that these chromium-rich phases increase the sensitivity to pitting corrosion and the difficulty of repairing passive film on the SS surface.[97]

4.3. Water Condition in DWDS. *4.3.1. Chloride Ions and Free Chlorine.* Although SS can form passive film to avoid further corrosion, the passive film is sensitive to chloride ions, which are the main cause of pitting corrosion and crevice corrosion in DWDS. When chloride ions attack the passive film, they penetrate the film along paths between nanocrystals and amorphous regions (i.e., the two phases are generated during passive film formation), finally reaching the interface between the SS substrate and passive film (Figure 5a). Such chloride ion attack results in the creation of a microscopically uneven interface structure and the initiation of corrosion pits.[47] On the other hand, free chlorine tends to non-homogeneously adsorb on the bare metal surface and accept electrons from either SS substrate or oxidized ferrous ions, leading to the formation of FeO, α-FeOOH, γ-FeOOH, Fe_2O_3, Fe_3O_4, CrOOH, and Cr_2O_3 in DWDS. This process leads to the formation of concave sites that facilitate chloride permeation, thereby amplifying corrosion.[98] Compared with the downstream SS pipe in DWDS, the area surrounding the dosing point in the drinking water treatment plant tends to cause severe SS corrosion due to the release of free chlorine.[99] Additionally, as described in Section 3.1, free chlorine can directly react with Cr(0) and lead to the formation of Cr(VI), which negatively impacts the water quality in DWDS.

4.3.2. Dissolved Oxygen. The corrosion rate of SS is significantly impacted by the presence of dissolved oxygen in DWDS. When the passive film of SS is penetrated, dissolved oxygen will participate in the electrochemical cell reaction and facilitate the oxidation of SS. As the dissolved oxygen level becomes higher, both anodic reaction from the corrosion initiation points and cathodic process on the SS passive film will be accelerated.[48] Figure 5b illustrates the range of perfect passivation, which is defined by the difference between repassivation potential and pitting potential ($E_{rp}-E_{corr}$).[100−102] Within the range of perfect passivation, the pit initiation and propagation of existing pits are inhibited. As the dissolved oxygen concentration rises, the range of perfect passivation gradually diminishes, indicating a decreasing trend on corrosion resistance. Additionally, the stability of the passive film is also influenced by the dissolved oxygen. Dissolved oxygen tends to be adsorbed into oxygen vacancies (i.e., point defects on the passive film), hindering the annihilation of oxygen vacancies during passive film formation. As dissolved oxygen concentration transitions from low to high, the gradual increase in oxygen vacancies can deteriorate the passive film.[103−105] Taken together, it is imperative to avoid excessive dissolved oxygen in DWDS to inhibit further SS corrosion.

4.3.3. pH. pH influences the pitting corrosion of SS via affecting the passivity breakdown potential (E_{bd}) and corrosion potential (E_{corr}) of SS. Pitting corrosion occurs when E_{corr} is higher than E_{bd},[106] and a larger disparity between E_{corr} and E_{bd} reduces the likelihood of pit initiation. An example of the pH impact on $E_{bd}-E_{corr}$ is presented in Figure 5c under conditions of a fixed chloride content of 1000 mg L^{-1} and a temperature of 20 °C. As the pH value rises, $E_{bd}-E_{corr}$ gradually increases, subsequently contributing to the gradual improvement in the corrosion resistance of SS.[49,107] Additionally, regarding the impact of pH on the SS passive film, the film thickness displays an obvious linear increment with an increasing pH value. When the passive film thickens, the corrosion resistance of SS is enhanced.[108] As the pH rises from 6 to 8, Cr(III)−Fe(III) hydroxides undergo a higher extent of hydroxylation, indicating lower redox activity with chlorine and releasing less Cr(VI) into the water.[109] Therefore, maintaining a subalkaline environment in the DWDS is of great importance for preventing SS corrosion and water contamination.

4.3.4. Temperature. Water temperature exhibits a strong association with the SS corrosion rate.[110] In the presence of chloride, higher temperature can expedite the process of pit initiation by facilitating the transition from a metastable to a stable condition for pits.[106,111,112] The influence of temperature on the $E_{bd}-E_{corr}$ value of SS is presented in Figure 5d. Rising the temperature renders a decreased $E_{bd}-E_{corr}$ value, indicating an increasing tendency for corrosion. It is worth noting that when the temperature exceeds 40 °C, the slope of the curve decreases, and the impact of temperature on SS corrosion tends to stabilize. Additionally, the strength of the SS passive film diminishes with rising temperature.[49] With increasing temperature, the passive film is observed to exhibit greater porosity, thereby weakening its protective capabilities.[113] Given the operating temperature range of water pumps (40−60 °C) in DWDS, it is crucial to pay attention to SS corrosion prevention in high-temperature environment.

4.3.5. Flow Rate. The flow rate in DWDS is a critical factor for SS corrosion. SS pipes receive both radial and lateral fluid shocks during the DWDS operation. The critical flow rate for corrosion-induced damage in 304 SS typically ranges from 9 to 12 m s^{-1} [a commonly used jet impingement equipment was applied, testing conditions involving a 90° impact angle, a 3 mm jet nozzle, and a 5 mm standoff distance, using a 3.5% NaCl solution with 2 wt % silica sand (75−150 mesh)].[114−116] Exceeding this threshold results in a significant acceleration of the SS material degradation. Although the passive film may be damaged at flow rates as low as 0.6−2.8 m s^{-1}, it can maintain its protective function through dynamic self-repair. Therefore, the threshold for erosion-corrosion can reach as high as 9−12 m s^{-1}.[22] However, it is worth noting that mechanical fracture may still occur on SS at lower water flow velocities.[117] Under the influence of SO_4^{2-} and Cl^-, regrowing the passive film to its initial state within a limited time is challenging, thereby elevating the risk of corrosion in lower water flow rates. Figure 5e illustrates the influence of water flow intensity on SS corrosion at various hydraulic heights,[118] which can reflect the impact of flow rate on SS pipe corrosion, with the liquid distributor operating at 1 m/s. A higher N_D signifies increased oxygen vacancies or cation vacancies in the passive film, which make SS more susceptible to corrosion. As the vertical hydraulic height increases, N_D increases and renders a greater potential for SS corrosion.

https://doi.org/10.1021/acsestengg.5c00260
ACS EST Engg. XXXX, XXX, XXX−XXX

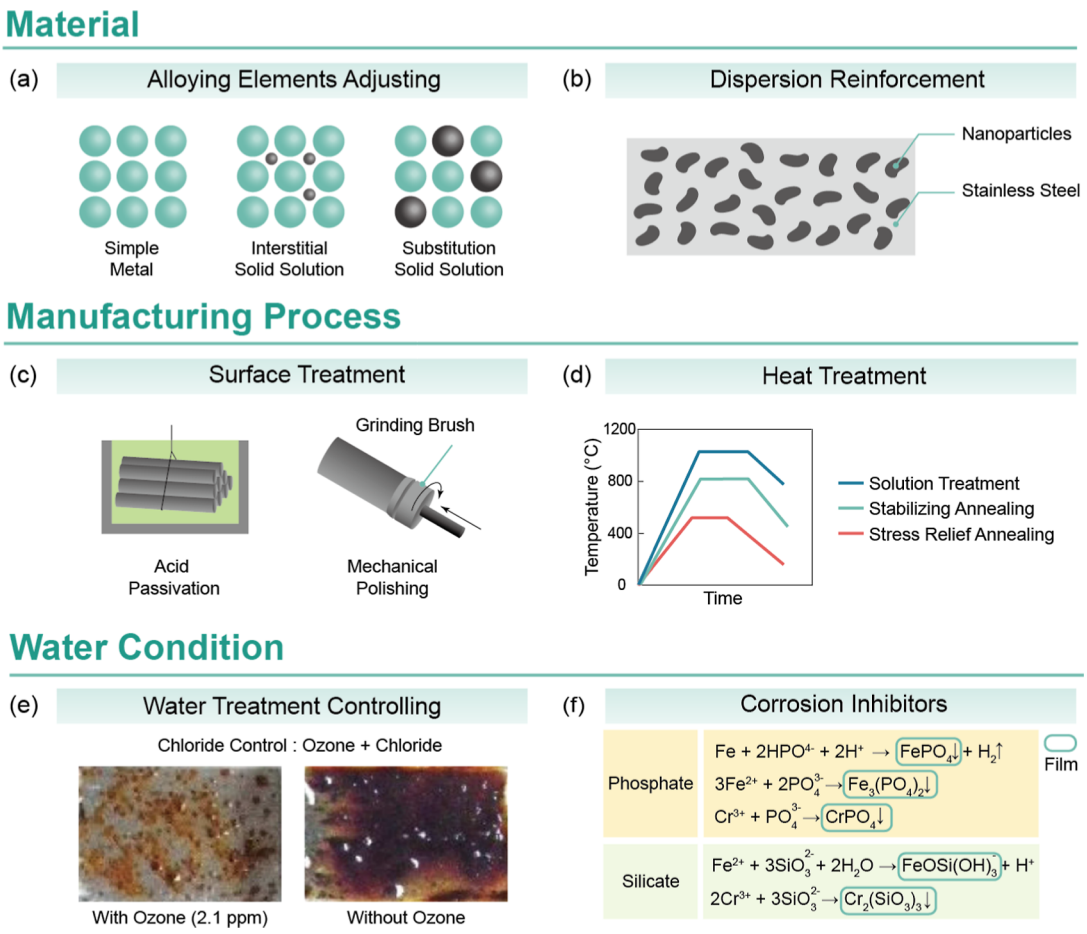

Figure 6. Approaches to prevent SS corrosion, including the aspects of material composition, manufacturing technique, and water conditions. (a) Additional metal elements for anticorrosion reinforcement, in which interstitial or substitutional solid solution is formed in SS. (b) Dispersion strengthening, i.e., strengthening is performed by introducing nanoparticles in base metal. (c) Surface treatment methods, including acid passivation by acid immersion and internal surface polishing by a grinding brush. (d) Heat treatment process, in which the heating temperature is programmed to change as a function of time. The heat treatment process mainly includes three stages: heating, holding, and cooling, which can be divided into various heat treatment methods according to different heating temperatures and cooling methods. (e) Adding ozone to chlorinated water as a water treatment control method to protect steel against corrosion.[172] Reproduced with permission from ref 172. Copyright 2012 Elsevier. (f) Addition of corrosion inhibitors, including phosphate and silicate for corrosion prevention. By generating $FePO_4$, $Fe_3(PO_4)_2$, $FeOSi(OH)_3^-$, $CrPO_4$, and $Cr_2(SiO_3)_3$, a protective film can be formed to mitigate SS corrosion.[177−179]

4.3.6. Sulfate. Sulfate demonstrates a crucial influence on SS corrosion. Its presence in DWDS primarily originates from two sources: (i) groundwater, which is likely to contain excessive sulfate or thiosulfate due to rock weathering.[119,120] (ii) Water treatment during which sulfate levels can be elevated by the dosing of sulfate-containing flocculant (common forms include $CaSO_4$, $MgSO_4$, Na_2SO_4, etc.). The impact of sulfate on SS corrosion is generally manifested in the strong acidic environment, while sulfate exhibits minimal impact in the neutral pH level.[108,121] However, the coexistence of both sulfate and SRB can trigger microbiologically induced corrosion of SS.[122] On the other hand, sulfate is also regarded as a contributing factor to heavy metal release in DWDS. Sulfate is not only related to increasing levels of Fe in the bulk water causing water discoloration but also rapidly triggers the release of heavy metals including Mn, Ni, Cu, Pb, Cr, and As from the corrosion scale.[88] Figure 5f illustrates the sulfate impact on Fe release from groundwater pipe with corrosion scale. The sulfate concentration increased from 75 to 300 mg L^{-1}, while the dissolved oxygen concentration gradually decreased from 6.67 to 3.65 mg L^{-1}. During this period, the concentration of released Fe increased by nearly 3-fold [the peak value exceeding 1 mg L^{-1}, which exceeds the standards for drinking water quality in China (0.3 mg L^{-1})]. The increase in the sulfate concentration leads to a relatively anaerobic environment in DWDS, then previously deposited ferric scale can act as an electron acceptor in the electrochemical corrosion and initiate ferrous iron release.[123] In this regard, the sulfate content in DWDS needs to be strictly controlled.

5. STRATEGIES FOR IMPROVING THE CORROSION RESISTANCE OF SS IN DWDS

5.1. Anticorrosion Strategies Based on the SS Material Composition. *5.1.1. Metal Alloying.* The corrosion resistance of SS in DWDS is primarily determined by its material properties, with alloying elements playing a crucial role in setting the upper limit of this resistance. While Cr is pivotal for passivating SS and improving its corrosion resistance,[124−127] simply increasing the Cr content is not a practical solution due to cost and processability. In this regard, beyond increasing the Cr content, adjusting the elemental composition through the formation of interstitial or substitu-

https://doi.org/10.1021/acsestengg.5c00260
ACS EST Engg. XXXX, XXX, XXX−XXX

tional solid solutions within the crystal lattice of SS emerges as an alternative strategy for enhancing SS corrosion resistance (Figure 6a). In particular, when compared with the molecular weight of Fe, elements with smaller molecular weights (e.g., N and C) are incorporated into SS as interstitial solid solutions, while elements with larger molecular weights (e.g., Cr, Ni, Mo) exist in the form of substitutional solid solutions.[128−132]

The addition of Ni, Mo, N, Si, W, Ti, Nb, and Cu enhances SS corrosion resistance through mechanisms, including strengthening the passive film of SS and tuning its microstructure. First, the inclusion of Ni, Mo, N, and Si improves SS corrosion resistance by fortifying the strength of the SS passive film. Ni mitigates the electrochemical corrosion via increasing the low-frequency electrical resistance of the passive film,[133,134] while the solid solution of N within the steel matrix facilitates the repassivation of the passive film.[135,136] Mo contributes to the formation of a molybdenum-rich oxide stable film, serving as an effective barrier preventing the intrusion of detrimental halogen ions.[137,138] Similarly, an increased Si content in SS improves oxidation resistance and fosters the development of a uniform passive film.[139] Second, W, Ti, and Ni facilitate the SS corrosion resistance by tuning the microstructure of SS. The presence of W hinders the pitting corrosion by delaying the emergence of the detrimental intermetallic compounds during thermal cycles (i.e., σ-phase and χ-phase, which significantly lower the SS corrosion resistance. For specific information, see Table S5).[140,141] Ti and Nb in SS promote the preferential formation of TiC and NbC rather than Cr_7C_3 or $Cr_{23}C_6$, preventing intergranular corrosion by avoiding Cr depletion.[142,143] Third, the effect of Cu on corrosion is nuanced. Cu exhibits a tendency to decrease its dissolution rate in an acidic chloride solution, thus reducing the pitting propagation rate. Additionally, in sulfur-induced pitting corrosion, the formation of insoluble CuS can prohibit the initiation of pits. However, high concentration of Cu (wt % $\geq$ 1.58) leads to the emergence of the ε-phase in SS (an intermetallic compound which increases the hardness of SS and is thus detrimental to the passive film. For specific information, see Table S5), thereby reducing SS corrosion resistance.[144,145] Furthermore, elements such as C, Mn, and S, which were previously noted for their detrimental effects on corrosion resistance, should be minimized.

5.1.2. Dispersion Reinforcement. Dispersion reinforcement is promising for enhancing SS corrosion resistance by uniformly incorporating hard particles into SS, which form ultrafine second phases that are insoluble in the base metal.[146] Introducing nanosized Y_2O_3 or $Y_2Ti_2O_7$ (<50 nm) into SS through oxide-dispersed strengthening (ODS) demonstrates significant enhancement in corrosion resistance (Figure 6b, see the chemical compositions of ODS 304 SS and ODS 316 SS in Table S6).[147−149] In the ODS SS, dispersed Y−Ti−O particles, formed due to the addition of Ti in SS, serve as nucleation sites for oxides. This reduces the amount of Cr required to form Cr_2O_3, thereby enabling the formation of a passive film in alloys with lower Cr content.[148,150,151] Additionally, the smaller grain size of the ODS SS promotes the formation of a Cr-rich oxide layer in SS. This is because shorter grain boundaries can function as "short-circuits" for ions to pass through, allowing for rapid diffusion of Cr in ODS steel during the repassivation process, thus facilitating the formation of Cr_2O_3 in passive films.[152]

5.2. Anticorrosion Strategies Based on SS Manufacturing. *5.2.1. Surface Treatment and Structural Optimization of SS.* Surface treatment of SS is crucial for establishing a uniform and stable passive film as the untreated passive film is susceptible to damage due to residual rust from raw material and slag deposited on the SS surface during the welding process. In this regard, acid pickling serves as an effective approach to remove surface impurities such as rust, oxidation scales, and stains on SS. Given the higher reactivity with iron oxide than chromium oxide, acid pickling aids in eliminating chromium-depleted regions and thus enhances the corrosion resistance of SS.[153,154] After acid pickling, which lays the foundation for a better surface condition, acid passivation can be conducted to form a uniform passive film. Acid passivation utilizes a mild oxidant (e.g., nitric acid solution) to eliminate free iron or other foreign materials, facilitating the formation of the passive film.[155,156] Specifically, SS pipes can be grouped together during acid passivation and submerged in an acidic tank to form the passive film (Figure 6c).

Polishing SS to eliminate surface defects also serves as a corrosion-resistant measure. After processes such as casting, forging, and heat treatment, the SS surface will develop an iron oxide layer. If left untreated, the iron oxide layer may lead to further expansion of oxidization.[96] When the surface of SS is rough or contains scratches, such defects may also initiate corrosion.[157] To remove such defects, mainstream SS surface polishing methods include mechanical polishing, electrochemical polishing, and laser polishing. Mechanical polishing uses friction to remove surface metal,[158] while electrochemical polishing immerses SS in a suitable bath (e.g., sulfuric acid and orthophosphoric acid) for anodic dissolution under external current.[159] Laser polishing applies short laser pulses to melt and resolidify a very thin surface layer in order to achieve a smoother surface finish.[160] Among these techniques, the cost-effective mechanical polishing is widely used for SS pipe surface polishing, namely, applying the grinding brush at a high rotation speed inside the pipe for the inner surface polishing (Figure 6c). The polished SS surface can thus prevent the accumulation of deposits and the generation of surface crevices, thereby facilitating anticorrosion.

Beyond SS surface treatment, preventing the formation of crevices is an alternative and effective approach to inhibit crevice corrosion of SS. Crevice corrosion is initiated at crevices of metal−metal and metal-nonmetal junctions at ranges from 0.1 to 100 μm,[16] such as connection points of flange and welds with flaws (e.g., flaws induced by slag inclusion and incomplete fusion).[161] Effective prevention of crevices necessitates precautionary measures implemented throughout the manufacturing and installation processes of SS, including grinding and polishing the weld during manufacturing, employing low sulfur rubber gaskets for connections during pipe installation, and applying suitable non-contaminating fillers to cover crevices.

5.2.2. Heat Treatment of SS. Heat treatment achieves grain refinement and alleviation of residual stress, which are crucial for preventing SS corrosion triggered by uneven thermal effects or concentrated stress in SS manufacturing and installation. Typical heat treatment methods include solution treatment, stabilization annealing, and stress relief annealing. The main difference among these methods lies in the heating temperature (i.e., solution treatment > stabilization annealing > stress relief annealing), while other differences like holding time and cooling rate mainly depend on the SS size (Figure 6d). First, in the solution treatment, heating facilitates the fusion of chromium-rich carbides (Cr_7C_3 and $Cr_{23}C_6$) and σ phase

https://doi.org/10.1021/acsestengg.5c00260
ACS EST Engg. XXXX, XXX, XXX−XXX

(an intermetallic compound which increases hardness and decreases toughness and elongation of SS. For specific information, see Table S5) from SS grain boundary into grain, preventing chromium depletion in passive film and thus increasing SS corrosion resistance.[142,143] Second, stabilization annealing is specifically applied for treating SS containing Ti and Nb. To ensure that carbon in the SS predominantly forms TiC and NbC rather than Cr_7C_3 and $Cr_{23}C_6$, the annealing temperature should be above the melting points of Cr_7C_3 and $Cr_{23}C_6$ while below the melting points of TiC and NbC, thus preventing the depletion of Cr in grain boundary.[162,163] Third, stress relief annealing is conducted by heating the SS workpiece below the recrystallization temperature to release residual stresses generated during manufacturing. This process reduces the cracking tendency of SS without altering its internal phases.

5.2.3. Surface Modification of SS. Surface modification improves SS corrosion resistance via enhancing surface smoothness and decreasing surface corrosion current.[164] Coating SS surfaces with metal nitrides, metal oxides, functionalized materials, and surface nitriding are proven effective in anticorrosion.[165] Metal nitrides, including TiN, (TiAl)N, and CrN, coated by physical vapor deposition, not only enable wear-resistant and antifriction performance for SS surface which mitigate water flow impact but also provide anticorrosion property. These metal nitride coatings are chemically inert and consequently have a high corrosion potential, preventing SS from corroding. The corrosion resistance sequence of TiN, (TiAl)N, and CrN in NaCl solution is CrN > (TiAl)N > TiN > 304 SS (Figure S7).[166] Metal oxides, such as TiO_2, SiO_2, and Al_2O_3, have also been utilized for SS surface modification via physical vapor deposition. These ceramic coatings provide effective electrical insulation, thereby minimizing corrosion current.[167−170] Surface nitriding is another technique used in SS corrosion control, which forms a nitriding layer as nitrogen atoms penetrate the surface of the SS surface. Nitrogen atoms tend to accumulate on the SS surface and thus inhibit the dissolution of fresh metal.[171]

5.3. Anticorrosion Strategies Based on DWDS Water Condition. *5.3.1. Upstream Drinking Water Treatment.* The decisive cause of SS corrosion is the residual chloride in DWDS for maintaining disinfection. Alternative disinfection technologies are sought for reducing chloride amount and enhancing SS corrosion resistance, in which ozonation offers a promising and sustainable approach. As shown in Figure 6e, steel showcases heightened corrosion resilience in ozonized water. Ozone fosters the formation of a compact and thin passive film on the SS surface, which increases charge transfer resistance and thus reduces the anodic corrosion current in the presence of chloride. Briefly, by adsorbing on the SS surface, ozone undergoes transformation into oxygen radical (O*), which reacts with the released electron from iron corrosion reaction to yield O^{2-}. The generated O^{2-} subsequently coalesces with Fe, Mg, and Ca cations, leading to the formation of a compact and thin passive film on the SS surface. This passive film, comprised components such as Fe_3O_4 and $CaCO_3$, imparts heightened stability to corrosion scales, effectively inhibiting corrosion and iron release.[172,173] Considering the inactivation efficiency of *E. coli*, it is found that, compared to chlorination alone, pretreatment with ozone can enhance the disinfection efficiency of chlorine by 2.4% to 18.5%.[174] The synergistic effect is mainly attributed to the removal of chlorine-consuming substances by ozone. In this regard, the synergistic effect of ozone and chlorine can protect SS surface while enhancing disinfection effectiveness, reducing the required chlorine dosage, and contributing to an improvement in water quality.[175] Apart from chlorine, considering the higher sulfate content in groundwater, water treatment processes including ion exchange, actived carbon adsorption, electrocoagulation, electrodialysis, nanofiltration, and double-membrane processes can also be used to lower sulfate levels for alleviating SS corrosion.[176]

5.3.2. Corrosion Inhibitors. Dosing corrosion inhibitors can adjust the pH value and lower scaling tendencies, thus preventing the accumulation and diffusion of hazardous heavy metals from the scale. Commonly used corrosion inhibitors include phosphate, polyphosphate, orthophosphate, and silicate (Figure 6f).[177−179] The proper dosing of those inhibitors can meet corrosion prevention requirements without contamination of drinking water. Phosphate such as potassium zinc phosphate ($KZn_2PO_4(HPO_4)$) can impede both anodic and cathodic reactions by forming protective layers on the anodic and cathodic sites of SS surface, as shown in eqs 3−5.[178] Phosphate also adjusts the pH value to maintain an alkaline environment in DWDS,[180−183] which enhances the corrosion resistance as expounded in 4.3.3. Additionally, dosing silicate inhibitors can replace water molecules on the steel−liquid interface and form a more structured silicate film on the SS surface, thus reducing film defects and lowering ion migration through the film.[179,184,185] It is also worth noting that when adding corrosion inhibitors, the dosing limits should be reasonably controlled to avoid a secondary impact on water quality and the environment.

$$3Fe^{2+} + 2PO_4^{3-} \rightarrow Fe_3(PO_4)_2 \downarrow \text{(film precipitation on the anodic region)} \quad (3)$$

$$3Zn^{2+} + 2PO_4^{3-} \rightarrow Zn_3(PO_4)_2 \downarrow \text{(film precipitation on both anodic and cathodic regions)} \quad (4)$$

$$Zn^{2+} + 2OH^- \rightarrow Zn(OH)_2 \downarrow \text{(film precipitation on the cathodic region)} \quad (5)$$

6. CHALLENGES AND FUTURE PROSPECTS

6.1. Formation Mechanism of the Passive Film and the Impact of Repassivation on Water Quality. The resistance to corrosion of SS is primarily due to the presence of the chromium-rich passive film. The passive film on SS is crucial for its corrosion resistance and durability but its formation mechanism and the impact of repassivation in DWDS still remain unclear. The passive film on SS is composed of nanocrystals and an amorphous zone, where the formation of nanocrystals can create pathways for chloride ions within the passive film. In this regard, studying how to prevent the formation of nanocrystals within the passive film and ensuring the creation of a homogeneous, stable, and Cl-resistant passive film during passivation can significantly enhance the corrosion resistance of SS in DWDS. Additionally, the bypassivation process of SS involves a comprehensive physicochemical reaction process that includes Cr, which may cause water contamination. Further research is needed to

https://doi.org/10.1021/acsestengg.5c00260
ACS EST Engg. XXXX, XXX, XXX−XXX

understand the impact of the repassivation process on water quality and its influencing factors.

6.2. Impact of SS Production and Installation Processes on DWDS Water Quality. The corrosion resistance of SS requires the appropriate SS manufacturing techniques. Currently, defects such as crevices, incomplete fusion, cracks, slag inclusion, and harmful phases are potentially generated during the production and welding of SS facilities. These defects are the main initiation points of electrochemical corrosion of SS in the DWDS environment, leading to water pollution issues of heavy metal release. Currently, there is insufficient research on the impact of the manufacturing processes of SS on corrosion and heavy metal release from materials perspectives. Understanding the cascading effects from SS manufacturing to SS corrosion and then to heavy metal release in DWDS, and identifying targeted manufacturing processes to alleviate critical defects, is of paramount importance for the niche design of SS in DWDS.

6.3. Lifecycle Assessment and Techno-Economic Analysis of SS Pipe in DWDS. Beyond the prevalent use of 304 and 316 austenitic SS pipe materials, advancements in manufacturing processes and material performance render ferritic SS, duplex SS, and other types of austenitic SS increasingly viable for pipeline applications in DWDS. Additionally, emerging manufacturing techniques, including physical vapor deposition, laser processing, and ion beam treatment, have demonstrated the potential to enhance SS's anticorrosion performance through surface modification. Nonetheless, these emerging materials and methods face challenges related to cost-effectiveness, long-term stability, and environmental sustainability. In this regard, it is essential to evaluate emerging SS materials and SS with different manufacturing techniques for use in DWDS from a lifecycle assessment perspective, comprehensively considering material performance, operating environment, cost-effectiveness, and maintenance. This assessment could assist in elucidating the complex trade-offs between the enhanced functionality of SS pipes, the additional environmental burden they may impose, and their techno-economic efficiency over the entire lifecycle, using 304 and 316 austenitic SS as benchmarks. Further, this evaluation could facilitate the application of proper SS materials in DWDS and promote the development of greener, more cost-effective, and efficient anticorrosion techniques of SS pipes.

■ ASSOCIATED CONTENT

Supporting Information

The Supporting Information is available free of charge at https://pubs.acs.org/doi/10.1021/acsestengg.5c00260.

Pitting resistance equivalent number (PREN); classification of SS; elemental compositions of SS; chemical equations involved in the scale formation process; characterization of inorganic contamination in scales; detrimental intermetallic compounds in SS; chemical compositions of ODS 304 SS and ODS 316 SS (wt %); SEM images of intergranular attack on AISI 321 SS; inspection of corrosion in pipe welding; SEM image of SS corrosion scale cracks; illustration of chloride attack on the SS passive film; perfect (E_{rp}−E_{corr}) and imperfect passivity (E_p−E_{rp}) ranges for 2205 duplex SS in the hot concentrated seawater with different dissolved oxygen level; total iron release of pipelines under different sulfate concentrations; and free corrosion potential vs time for coated and uncoated 304 SS in 0.5 M NaCl solution (PDF)

■ AUTHOR INFORMATION

Corresponding Authors

Yumeng Zhao − *State Key Laboratory of Urban Water Resource and Environment, Harbin Institute of Technology, Harbin 150090, China;* orcid.org/0000-0002-9279-8501; Email: zhaoyumeng@hit.edu.cn

Gang Liu − *State Key Laboratory of Environmental Aquatic Chemistry, Research Center for Eco-Environmental Sciences, Chinese Academy of Sciences, Beijing 100085, China; Section of Sanitary Engineering, Department of Water Management, Faculty of Civil Engineering and Geosciences, Delft University of Technology, Delft 2628 CN, The Netherlands;* orcid.org/0000-0002-4008-9017; Email: g.liu-1@tudelft.nl

Authors

Xinyu Pan − *State Key Laboratory of Urban Water Resource and Environment, Harbin Institute of Technology, Harbin 150090, China; State Key Laboratory of Precision Welding & Joining of Materials and Structures, Harbin Institute of Technology, Harbin 150006, China*

Xuhui Dang − *State Key Laboratory of Urban Water Resource and Environment, Harbin Institute of Technology, Harbin 150090, China;* orcid.org/0009-0006-2885-4587

Meng Sun − *State Key Laboratory of Environmental Aquatic Chemistry, Research Center for Eco-Environmental Sciences, Chinese Academy of Sciences, Beijing 100085, China;* orcid.org/0000-0002-8188-9264

Gang Wen − *Shaanxi Key Laboratory of Environmental Engineering, Xi'an University of Architecture and Technology, Xi'an 710055, China*

Xinlei Li − *State Key Laboratory of Precision Welding & Joining of Materials and Structures, Harbin Institute of Technology, Harbin 150006, China*

Ao Chen − *State Key Laboratory of Precision Welding & Joining of Materials and Structures, Harbin Institute of Technology, Harbin 150006, China*

Chotiwat Jantarakasem − *Department of Mechanical Engineering, Massachusetts Institute of Technology, Cambridge, Massachusetts 02139, United States*

Federick Pinongcos − *Trussell Technologies, San Diego, California 9212, United States*

Linda Li − *Dillon Consulting Limited, Kitchener, Ontario N2H 5G5, Canada*

Jun Ma − *State Key Laboratory of Urban Water Resource and Environment, Harbin Institute of Technology, Harbin 150090, China;* orcid.org/0000-0002-0903-5547

Complete contact information is available at: https://pubs.acs.org/10.1021/acsestengg.5c00260

Notes

The authors declare no competing financial interest.

■ ACKNOWLEDGMENTS

This work was supported by the National Natural Science Foundation of China (No. 52200008 and No. 52270043), the Young Elite Scientists Sponsorship Program by CAST, and the

National Key Research and Development Program of China (2023YFE0113800).

REFERENCES

(1) Tong, H.; Zhao, P.; Zhang, H.; Tian, Y.; Chen, X.; Zhao, W.; Li, M. Identification and characterization of steady and occluded water in drinking water distribution systems. *Chemosphere* **2015**, *119*, 1141−1147.

(2) Rezayat, M.; Karamimoghadam, M.; Moradi, M.; Casalino, G.; Roa Rovira, J. J.; Mateo, A. Overview of Surface Modification Strategies for Improving the Properties of Metastable Austenitic Stainless Steels. *Metals* **2023**, *13* (7), 1268.

(3) Chao, Q.; Thomas, S.; Birbilis, N.; Cizek, P.; Hodgson, P. D.; Fabijanic, D. The effect of post-processing heat treatment on the microstructure, residual stress and mechanical properties of selective laser melted 316L stainless steel. *Mater. Sci. Eng., A* **2021**, *821*, 141611.

(4) Tuthill, A. H. Stainless-steel piping. *J. Am. Water Works Assn.* **1994**, *86* (7), 67−73.

(5) Cui, Y.; Liu, S.; Smith, K.; Yu, K.; Hu, H.; Jiang, W.; Li, Y. Characterization of corrosion scale formed on stainless steel delivery pipe for reclaimed water treatment. *Water Res.* **2016**, *88*, 816−825.

(6) Percival, S.; Knapp, J.; Edyvean, R.; Wales, D. Biofilms, mains water and stainless steel. *Water Res.* **1998**, *32* (7), 2187−2201.

(7) Han, Y.; Liu, Z.-H.; Wu, C.-B.; Zhao, Y.; Zu, G.-Q.; Zhu, W.-W.; Ran, X. A short review on the role of alloying elements in duplex stainless steels. *Tungsten* **2023**, *5* (4), 419−439.

(8) Luo, H.; Wang, X.; Liu, Z.; Yang, Z. Influence of refined hierarchical martensitic microstructures on yield strength and impact toughness of ultra-high strength stainless steel. *J. Mater. Sci. Technol.* **2020**, *51*, 130−136.

(9) Cui, P.; Xing, G.; Nong, Z.; Chen, L.; Lai, Z.; Liu, Y.; Zhu, J. Recent Advances on Composition-Microstructure-Properties Relationships of Precipitation Hardening Stainless Steel. *Materials* **2022**, *15* (23), 8443.

(10) Astafurov, S.; Astafurova, E. Phase composition of austenitic stainless steels in additive manufacturing: A review. *Metals* **2021**, *11* (7), 1052.

(11) Zinovieva, O.; Romanova, V.; Balokhonov, R. Effects of scanning pattern on the grain structure and elastic properties of additively manufactured 316L austenitic stainless steel. *Mater. Sci. Eng., A* **2022**, *832*, 142447.

(12) Liu, T.; Zheng, K.; Lin, Y.; Luo, Z. Effect of second-phase particles on the oxidation behaviour of a high-manganese austenitic heat-resistant steel. *Corros. Sci.* **2021**, *182*, 109284.

(13) Bach, A.-C.; Martin, F.; Duhamel, C.; Perrin, S.; Jomard, F.; Crepin, J. Hydrogen trapping by irradiation-induced defects in 316 L stainless steel: A combined experimental and modeling study. *J. Nucl. Mater.* **2022**, *562*, 153603.

(14) Li, W.; Zhang, J.; Xin, P.; Wen, Z.; Jing, H.; Zhao, L.; Xu, L.; Han, Y. Corrosion behavior of the heat affected zone in a 316 L pipeline weld. *Mater. Test.* **2021**, *63* (7), 617−622.

(15) Kong, D.; Dong, C.; Ni, X.; Zhang, L.; Yao, J.; Man, C.; Cheng, X.; Xiao, K.; Li, X. Mechanical properties and corrosion behavior of selective laser melted 316L stainless steel after different heat treatment processes. *J. Mater. Sci. Technol.* **2019**, *35* (7), 1499−1507.

(16) Costa, E. M.; Dedavid, B. A.; Santos, C. A.; Lopes, N. F.; Fraccaro, C.; Pagartanidis, T.; Lovatto, L. P. Crevice corrosion on stainless steels in oil and gas industry: A review of techniques for evaluation, critical environmental factors and dissolved oxygen. *Eng. Fail. Anal.* **2023**, *144*, 106955.

(17) Jandaghi, M. R.; Pouraliakbar, H.; Iannucci, L.; Fallah, V.; Pavese, M. Comparative assessment of gas and water atomized powders for additive manufacturing of 316 L stainless steel: Microstructure, mechanical properties, and corrosion resistance. *Mater. Charact.* **2023**, *204*, 113204.

(18) Li, N.; Wang, H.; Yin, H.; Liu, Q.; Tang, Z. Effect of temperature and impurity content to control corrosion of 316 stainless steel in molten KCl-$MgCl_2$ salt. *Materials* **2023**, *16* (5), 2025.

(19) Martínez-Aparicio, B.; Martínez-Bastidas, D.; Gaona-Tiburcio, C.; Martin, U.; Cabral-Miramontes, J.; Almeraya-Calderón, F. Localized corrosion of 15−5 PH and 17−4 PH stainless steel in NaCl solution. *J. Solid State Electrochem.* **2023**, *27* (11), 2993−3001.

(20) Shao, Z.; Yu, D.; Shao, D.; Du, Y.; Zheng, D.; Qiu, Z.; Wu, B. A protective role of Cl-ion in corrosion of stainless steel. *Corros. Sci.* **2024**, *226*, 111631.

(21) Wan, H.; Zhang, T.; Xu, Z.; Rao, Z.; Zhang, G.; Li, G.; Liu, H. Effect of sulfate reducing bacteria on the galvanic corrosion behavior of X52 carbon steel and 2205 stainless steel bimetallic couple. *Corros. Sci.* **2023**, *212*, 110963.

(22) Wang, Z.; Zheng, Y. Critical flow velocity phenomenon in erosion-corrosion of pipelines: Determination methods, mechanisms and applications. *J. Pipeline Sci. Eng.* **2021**, *1* (1), 63−73.

(23) Xiao, Q.; Chen, J.; Lee, H. B.; Jang, C.; Jang, K. Effect of heat treatment on corrosion behaviour of additively manufactured 316L stainless steel in high-temperature water. *Corros. Sci.* **2023**, *210*, 110830.

(24) Mameng, S. H.; Wegrelius, L.; Helmersson, B. Methods for Construction of Pitting Engineering Diagrams of Stainless Steels Used for Water Systems. In *Paper presented at the AMPP Annual Conference + Expo, AMPP CORROSION*; OnePetro: Denver, Colorado, USA, 2023.

(25) Liu, H.; Feng, C.; Wang, Z.; Zhang, Y.; Zhang, D.; Yan, Y. Study of fretting-initiated crevice corrosion and crevice corrosion affected fretting of stainless steel. *Corros. Sci.* **2023**, *225*, 111586.

(26) Fujii, T.; Suzuki, M.; Shimamura, Y. Susceptibility to intergranular corrosion in sensitized austenitic stainless steel characterized via crystallographic characteristics of grain boundaries. *Corros. Sci.* **2022**, *195*, 109946.

(27) Dong, L.; Ma, C.; Peng, Q.; Han, E.-H.; Ke, W. Microstructure and stress corrosion cracking of a SA508−309L/308L-316L dissimilar metal weld joint in primary pressurized water reactor environment. *J. Mater. Sci. Technol.* **2020**, *40*, 1−14.

(28) Tan, C.; Avasarala, S.; Liu, H. Hexavalent chromium release in drinking water distribution systems: new insights into zerovalent chromium in iron corrosion scales. *Environ. Sci. Technol.* **2020**, *54* (20), 13036−13045.

(29) Xu, X.; Liu, S.; Liu, Y.; Smith, K.; Cui, Y. Corrosion of stainless steel valves in a reverse osmosis system: analysis of corrosion products and metal loss. *Eng. Fail. Anal.* **2019**, *105*, 40−51.

(30) Dornhege, M.; Punckt, C.; Hudson, J. L.; Rotermund, H.-H. Spreading of corrosion on stainless steel: Simultaneous observation of metastable pits and oxide film. *J. Electrochem. Soc.* **2007**, *154* (1), C24.

(31) Tian, W.; Du, N.; Li, S.; Chen, S.; Wu, Q. Metastable pitting corrosion of 304 stainless steel in 3.5% NaCl solution. *Corros. Sci.* **2014**, *85*, 372−379.

(32) Li, W.; Ling, W.; Liu, S.; Zhao, J.; Liu, R.; Chen, Q.; Qiang, Z.; Qu, J. Development of systems for detection, early warning, and control of pipeline leakage in drinking water distribution: A case study. *J. Environ. Sci.* **2011**, *23* (11), 1816−1822.

(33) Liu, J.; Shentu, H.; Chen, H.; Ye, P.; Xu, B.; Zhang, Y.; Bastani, H.; Peng, H.; Chen, L.; Zhang, T. Change regularity of water quality parameters in leakage flow conditions and their relationship with iron release. *Water Res.* **2017**, *124*, 353−362.

(34) Zhang, S.; Tian, Y.; Guo, Y.; Shan, J.; Liu, R. Manganese release from corrosion products of cast iron pipes in drinking water distribution systems: Effect of water temperature, pH, alkalinity, SO_4^{2-} concentration and disinfectants. *Chemosphere* **2021**, *262*, 127904.

(35) Li, M.; Wang, Y.; Liu, Z.; Sha, Y.; Korshin, G. V.; Chen, Y. Metal-release potential from iron corrosion scales under stagnant and active flow, and varying water quality conditions. *Water Res.* **2020**, *175*, 115675.

(36) Chen, Y.; Zhou, H.; Gao, H.; Su, Z.; Li, X.; Qi, P.; Li, T.; Hu, C.; Li, Z.; Bi, Z.; et al. Comprehensive comparison of water quality risk and microbial ecology between new and old cast iron pipe distribution systems. *J. Environ. Sci.* **2024**, *146*, 55−66.

https://doi.org/10.1021/acsestengg.5c00260
ACS EST Engg. XXXX, XXX, XXX−XXX

(37) Li, M.; Liu, Z.; Chen, Y. Physico-chemical characteristics of corrosion scales from different pipes in drinking water distribution systems. *Water* **2018**, *10* (7), 931.
(38) Cai, M.; Zhao, Z.; Sun, W.; Yin, W.; Zhang, Y.; He, S. Impact of pipeline materials on water quality stability of desalinated seawater in the pipeline network. *Desalination* **2023**, *556*, 116558.
(39) Bi, H. Y.; Kokawa, H.; Wang, Z. J.; Shimada, M.; Sato, Y. S. Suppression of chromium depletion by grain boundary structural change during twin-induced grain boundary engineering of 304 stainless steel. *Scr. Mater.* **2003**, *49* (3), 219−223.
(40) Olsson, C.-O.; Landolt, D. Passive films on stainless steels—chemistry, structure and growth. *Electrochim. Acta* **2003**, *48* (9), 1093−1104.
(41) Wang, L.; Seyeux, A.; Marcus, P. Thermal stability of the passive film formed on 316L stainless steel surface studied by ToF-SIMS. *Corros. Sci.* **2020**, *165*, 108395.
(42) Wurzler, N.; Schutter, J. D.; Wagner, R.; Dimper, M.; Lützenkirchen-Hecht, D.; Ozcan, O. Abundance of Fe (III) during cultivation affects the microbiologically influenced corrosion (MIC) behaviour of iron reducing bacteria Shewanella putrefaciens. *Corros. Sci.* **2020**, *174*, 108855.
(43) Wu, X.; Liu, Y.; Sun, Y.; Dai, N.; Li, J.; Jiang, Y. A discussion on evaluation criteria for crevice corrosion of various stainless steels. *J. Mater. Sci. Technol.* **2021**, *64*, 29−37.
(44) Calabokis, O. P.; de la Rosa, Y. N.; Lepienski, C. M.; Cardoso, R. P.; Borges, P. C. Crevice and pitting corrosion of low temperature plasma nitrided UNS S32750 super duplex stainless steel. *Surf. Coat. Technol.* **2021**, *413*, 127095.
(45) Sun, Y.; Tan, X.; Lan, R.; Ran, G.; Li, J.; Jiang, Y. Mechanisms of inclusion-induced pitting of stainless steels: A review. *J. Mater. Sci. Technol.* **2024**, *168*, 143−156.
(46) Li, K.; Sun, L.; Cao, W.; Chen, S.; Chen, Z.; Wang, Y.; Li, W. Pitting corrosion of 304 stainless steel in secondary water supply system. *Corros. Commun.* **2022**, *7*, 43−50.
(47) Zhang, B.; Wang, J.; Wu, B.; Guo, X.; Wang, Y.; Chen, D.; Zhang, Y.; Du, K.; Oguzie, E.; Ma, X. Unmasking chloride attack on the passive film of metals. *Nat. Commun.* **2018**, *9* (1), 2559.
(48) Feng, Z.; Cheng, X.; Dong, C.; Xu, L.; Li, X. Effects of dissolved oxygen on electrochemical and semiconductor properties of 316L stainless steel. *J. Nucl. Mater.* **2010**, *407* (3), 171−177.
(49) Dastgerdi, A. A.; Brenna, A.; Ormellese, M.; Pedeferri, M.; Bolzoni, F. Experimental design to study the influence of temperature, pH, and chloride concentration on the pitting and crevice corrosion of UNS S30403 stainless steel. *Corros. Sci.* **2019**, *159*, 108160.
(50) Mou, L.; Bian, T.; Zhang, S.; Liu, B.; Wu, P.; Zhang, J.; Yu, Y.; Zhang, Y.; Wang, X. New sights on intergranular corrosion resistance mechanism of type 304 austenitic stainless steel by adjusting carbon contents. *J. Mater. Res. Technol.* **2023**, *26*, 666−680.
(51) Zhang, Y.; Cheng, S.; Wu, S.; Cheng, F. The evolution of microstructure and intergranular corrosion resistance of duplex stainless steel joint in multi-pass welding. *J. Mater. Process. Technol.* **2020**, *277*, 116471.
(52) Gupta, R. K.; Parvathavarthini, N.; Vinod Kumar, A.; Dayal, R. Influence of inclusion and specimen orientations on intergranular corrosion testing of AISI 316LN stainless steel. *Trans. Indian Inst. Met.* **2011**, *64*, 365−375.
(53) Wang, Y. D.; Peng, R. L.; Wang, X.-L.; McGreevy, R. L. Grain-orientation-dependent residual stress and the effect of annealing in cold-rolled stainless steel. *Acta Mater.* **2002**, *50* (7), 1717−1734.
(54) Nivas, R.; Das, G.; Das, S.; Mahato, B.; Kumar, S.; Sivaprasad, K.; Singh, P.; Ghosh, M. Effect of stress relief annealing on microstructure & mechanical properties of welded joints between low alloy carbon steel and stainless steel. *Metall. Mater. Trans. A* **2017**, *48*, 230−245.
(55) Adesanmi, A.; Omiogbemi, I. M.-B.; Gukop, N. S.; Gummadi, A. K.; Negash, S. M.; Dagwa, I. M. Microstructural and Corrosion Characteristics of a Heat Treatable Stainless-SteelWeldments. *IOP Conf. Ser.: Mater. Sci. Eng.* **2021**, *1185*, 012030.
(56) Huang, X.-z.; Wang, D.; Yang, Y.-t. Effect of precipitation on intergranular corrosion resistance of 430 ferritic stainless steel. *J. Iron Steel Res. Int.* **2015**, *22* (11), 1062−1068.
(57) Ng, D.-Q.; Chen, C.-Y.; Lin, Y.-P. A new scenario of lead contamination in potable water distribution systems: Galvanic corrosion between lead and stainless steel. *Sci. Total Environ.* **2018**, *637*, 1423−1431.
(58) Al Hossani, H.; Saber, T.; Mohammed, R.; El Din, A. S. Galvanic corrosion of copper-base alloys in contact with molybdenum-containing stainless steels in Arabian Gulf water. *Desalination* **1997**, *109* (1), 25−37.
(59) Xu, Y.; Hou, X.; Shi, Y.; Zhang, W.; Gu, Y.; Feng, C.; Volodymyr, K. Correlation between the microstructure and corrosion behaviour of copper/316 L stainless-steel dissimilar-metal welded joints. *Corros. Sci.* **2021**, *191*, 109729.
(60) Ng, D.-Q.; Lin, J.-K.; Lin, Y.-P. Lead release in drinking water resulting from galvanic corrosion in three-metal systems consisting of lead, copper and stainless steel. *J. Hazard. Mater.* **2020**, *398*, 122936.
(61) Okonkwo, B. O.; Ming, H.; Zhang, Z.; Wang, J.; Rahimi, E.; Hosseinpour, S.; Davoodi, A. Microscale investigation of the correlation between microstructure and galvanic corrosion of low alloy steel A508 and its welded 309/308L stainless steel overlayer. *Corros. Sci.* **2019**, *154*, 49−60.
(62) Dong, C.; Xiao, K.; Li, X.; Cheng, Y. Erosion accelerated corrosion of a carbon steel-stainless steel galvanic couple in a chloride solution. *Wear* **2010**, *270* (1−2), 39−45.
(63) Ryl, J.; Wysocka, J.; Darowicki, K. Determination of causes of accelerated local corrosion of austenitic steels in water supply systems. *Constr. Build. Mater.* **2014**, *64*, 246−252.
(64) Cui, L.; Xiaogang, L.; Chaofang, D. Pitting and galvanic corrosion behavior of stainless steel with weld in wet-dry environment containing Cl^-. *J. Univ. Sci. Technol. Beijing* **2007**, *14* (6), 517−522.
(65) Martins, C.; Moreira, J.; Martins, J. Corrosion in water supply pipe stainless steel 304 and a supply line of helium in stainless steel 316. *Eng. Fail. Anal.* **2014**, *39*, 65−71.
(66) Tawancy, H.; Al-Hadhrami, L. M. Case study: pitting and stress corrosion cracking in heat-affected zone of welded underground 304 stainless steel pipe. *J. Mater. Eng. Perform.* **2012**, *21*, 1757−1762.
(67) Dong, L.; Peng, Q.; Han, E.-H.; Ke, W.; Wang, L. Stress corrosion cracking in the heat affected zone of a stainless steel 308L-316L weld joint in primary water. *Corros. Sci.* **2016**, *107*, 172−181.
(68) Zhu, R.; Wang, J.; Zhang, L.; Zhang, Z.; Han, E.-h. Stress corrosion cracking of 316L HAZ for 316L stainless steel/Inconel 52M dissimilar metal weld joint in simulated primary water. *Corros. Sci.* **2016**, *112*, 373−384.
(69) Li, Y.; Ning, C. Latest research progress of marine microbiological corrosion and bio-fouling, and new approaches of marine anti-corrosion and anti-fouling. *Bioact. Mater.* **2019**, *4*, 189−195.
(70) Ziadi, I.; Alves, M.; Taryba, M.; El-Bassi, L.; Hassairi, H.; Bousselmi, L.; Montemor, M.; Akrout, H. Microbiologically influenced corrosion mechanism of 304L stainless steel in treated urban wastewater and protective effect of silane-TiO_2 coating. *Bioelectrochemistry* **2020**, *132*, 107413.
(71) Cui, Y.; Liu, S.; Smith, K.; Hu, H.; Tang, F.; Li, Y.; Yu, K. Stainless steel corrosion scale formed in reclaimed water: Characteristics, model for scale growth and metal element release. *J. Environ. Sci.* **2016**, *48*, 79−91.
(72) Waanders, F.; Vorster, S.; Engelbrecht, A. Mössbauer and SEM characterisation of the scale on type 304 stainless steel. *Scr. Mater.* **2000**, *42* (10), 997−1000.
(73) Xu, X.; Liu, S.; Smith, K.; Cui, Y.; Wang, Z. An overview on corrosion of iron and steel components in reclaimed water supply systems and the mechanisms involved. *J. Cleaner Prod.* **2020**, *276*, 124079.
(74) Sherar, B.; Keech, P.; Shoesmith, D. Carbon steel corrosion under anaerobic-aerobic cycling conditions in near-neutral pH saline solutions-Part 1: Long term corrosion behaviour. *Corros. Sci.* **2011**, *53* (11), 3636−3642.

https://doi.org/10.1021/acsestengg.5c00260
ACS EST Engg. XXXX, XXX, XXX−XXX

(75) Sherar, B.; Keech, P.; Shoesmith, D. Carbon steel corrosion under anaerobic-aerobic cycling conditions in near-neutral pH saline solutions. Part 2: Corrosion mechanism. *Corros. Sci.* **2011**, *53* (11), 3643−3650.
(76) Zhang, H.; Tian, Y.; Kang, M.; Chen, C.; Song, Y.; Li, H. Effects of chlorination/chlorine dioxide disinfection on biofilm bacterial community and corrosion process in a reclaimed water distribution system. *Chemosphere* **2019**, *215*, 62−73.
(77) Wang, H.; Hu, C.; Hu, X.; Yang, M.; Qu, J. Effects of disinfectant and biofilm on the corrosion of cast iron pipes in a reclaimed water distribution system. *Water Res.* **2012**, *46* (4), 1070−1078.
(78) Xu, Q.; Gao, K.; Wang, Y.; Pang, X. Characterization of corrosion products formed on different surfaces of steel exposed to simulated groundwater solution. *Appl. Surf. Sci.* **2015**, *345*, 10−17.
(79) Little, B. J.; Gerke, T. L.; Lee, J. S. Mini-review: the morphology, mineralogy and microbiology of accumulated iron corrosion products. *Biofouling* **2014**, *30* (8), 941−948.
(80) Zhang, H.; Liu, D.; Zhao, L.; Wang, J.; Xie, S.; Liu, S.; Lin, P.; Zhang, X.; Chen, C. Review on corrosion and corrosion scale formation upon unlined cast iron pipes in drinking water distribution systems. *J. Environ. Sci.* **2022**, *117*, 173−189.
(81) Yang, L.; Bo, C.; Junwei, W.; Zhiping, W.; Wensheng, L. Corrosion behavior of Cr, Fe and Ni based superalloy in molten NaCl. *Rare Metal Mater. Eng.* **2014**, *43* (1), 17−23.
(82) Sugae, K.; Kamimura, T.; Asakura, R.; Doi, T.; Miyuki, H.; Kudo, T. Electrochemical reduction and re-oxidation behavior of α, β, and γ-iron oxy-hydroxide films on electrodes. *Mater. Corros.* **2019**, *70* (2), 187−196.
(83) Lair, V.; Antony, H.; Legrand, L.; Chaussé, A. Electrochemical reduction of ferric corrosion products and evaluation of galvanic coupling with iron. *Corros. Sci.* **2006**, *48* (8), 2050−2063.
(84) Xu, X.; Liu, S.; Liu, Y.; Smith, K.; Wang, X.; Li, J.; Ma, Z.; Wang, Z.; Cui, Y. Water quality induced corrosion of stainless steel valves during long-term service in a reverse osmosis system. *J. Environ. Sci.* **2020**, *89*, 218−226.
(85) Hu, J.; Dong, H.; Xu, Q.; Ling, W.; Qu, J.; Qiang, Z. Impacts of water quality on the corrosion of cast iron pipes for water distribution and proposed source water switch strategy. *Water Res.* **2018**, *129*, 428−435.
(86) Peng, C.-Y.; Korshin, G. V.; Valentine, R. L.; Hill, A. S.; Friedman, M. J.; Reiber, S. H. Characterization of elemental and structural composition of corrosion scales and deposits formed in drinking water distribution systems. *Water Res.* **2010**, *44* (15), 4570−4580.
(87) Pan, L.; Li, G.; Li, J.; Gao, J.; Liu, Q.; Shi, B. Heavy metal enrichment in drinking water pipe scales and speciation change with water parameters. *Sci. Total Environ.* **2022**, *806*, 150549.
(88) Sun, H.; Shi, B.; Yang, F.; Wang, D. Effects of sulfate on heavy metal release from iron corrosion scales in drinking water distribution system. *Water Res.* **2017**, *114*, 69−77.
(89) Liu, G.; Zhang, Y.; Knibbe, W.-J.; Feng, C.; Liu, W.; Medema, G.; van der Meer, W. Potential impacts of changing supply-water quality on drinking water distribution: A review. *Water Res.* **2017**, *116*, 135−148.
(90) Lin, H.; Lin, H.; Fang, X.; Wang, M.; Huang, L. Intelligent pipeline leak detection and analysis system. In *2020 15th International Conference on Computer Science & Education (ICCSE)*, 2020; IEEE.
(91) Keramat, A.; Payesteh, M.; Brunone, B.; Meniconi, S. Interdependence of flow and pipe characteristics in transient induced contamination intrusion: numerical analysis. *J. Hydroinf.* **2020**, *22* (3), 473−490.
(92) Pardo, A.; Merino, M.; Coy, A.; Viejo, F.; Carboneras, M.; Arrabal, R. Influence of Ti, C and N concentration on the intergranular corrosion behaviour of AISI 316Ti and 321 stainless steels. *Acta Mater.* **2007**, *55* (7), 2239−2251.
(93) Sedriks, A. J. *Corrosion of Stainless Steels*; John Wiley & Sons, 1996.
(94) Meng, Q.; Frankel, G.; Colijn, H.; Goss, S. Stainless-steel corrosion and MnS inclusions. *Nature* **2003**, *424* (6947), 389−390.
(95) Lim, Y. S.; Kim, J. S.; Ahn, S. J.; Kwon, H. S.; Katada, Y. The influences of microstructure and nitrogen alloying on pitting corrosion of type 316L and 20 wt.% Mn-substituted type 316L stainless steels. *Corros. Sci.* **2001**, *43* (1), 53−68.
(96) Ress, J.; Monrrabal, G.; Díaz, A.; Pérez-Pérez, J.; Bastidas, J.; Bastidas, D. M. Microbiologically influenced corrosion of welded AISI 304 stainless steel pipe in well water. *Eng. Fail. Anal.* **2020**, *116*, 104734.
(97) Shi, Y.; Li, W.; Tian, L.; Sun, Y.; Zhang, J.; Jing, H.; Zhao, L.; Xu, L.; Han, Y. Effect of ferrite and grain boundary characteristics on corrosion properties of thermal simulated 316 L heat affected zone. *Corros. Sci.* **2023**, *222*, 111384.
(98) Zhang, H.; Zhao, L.; Liu, D.; Wang, J.; Zhang, X.; Chen, C. Early period corrosion and scaling characteristics of ductile iron pipe for ground water supply with sodium hypochlorite disinfection. *Water Res.* **2020**, *176*, 115742.
(99) Masters, S.; Wang, H.; Pruden, A.; Edwards, M. A. Redox gradients in distribution systems influence water quality, corrosion, and microbial ecology. *Water Res.* **2015**, *68*, 140−149.
(100) Zeng, H.; Yang, Y.; Zeng, M.; Li, M. Effect of dissolved oxygen on electrochemical corrosion behavior of 2205 duplex stainless steel in hot concentrated seawater. *J. Mater. Sci. Technol.* **2021**, *66*, 177−185.
(101) Bellezze, T.; Roventi, G.; Fratesi, R. Electrochemical characterization of three corrosion-resistant alloys after processing for heating-element sheathing. *Electrochim. Acta* **2004**, *49* (17−18), 3005−3014.
(102) Leiva-García, R.; Muñoz-Portero, M.; García-Antón, J. Corrosion behaviour of sensitized and unsensitized Alloy 900 (UNS 1.4462) in concentrated aqueous lithium bromide solutions at different temperatures. *Corros. Sci.* **2010**, *52* (3), 950−959.
(103) Kuang, W.; Wu, X.; Han, E.-H. Influence of dissolved oxygen concentration on the oxide film formed on 304 stainless steel in high temperature water. *Corros. Sci.* **2012**, *63*, 259−266.
(104) Cui, Z.; Chen, S.; Dou, Y.; Han, S.; Wang, L.; Man, C.; Wang, X.; Chen, S.; Cheng, Y. F.; Li, X. Passivation behavior and surface chemistry of 2507 super duplex stainless steel in artificial seawater: Influence of dissolved oxygen and pH. *Corros. Sci.* **2019**, *150*, 218−234.
(105) Zhang, Y.; Urquidi-Macdonald, M.; Engelhardt, G. R.; Macdonald, D. D. Development of localized corrosion damage on low pressure turbine disks and blades: I. Passivity. *Electrochim. Acta* **2012**, *69*, 1−11.
(106) Pardo, A.; Otero, E.; Merino, M.; López, M.; Utrilla, M.; Moreno, F. Influence of pH and chloride concentration on the pitting and crevice corrosion behavior of high-alloy stainless steels. *Corrosion* **2000**, *56* (04), 411−418.
(107) Li, L.; Dong, C.; Xiao, K.; Yao, J.; Li, X. Effect of pH on pitting corrosion of stainless steel welds in alkaline salt water. *Constr. Build. Mater.* **2014**, *68*, 709−715.
(108) Li, D.; Wang, J.; Chen, D.; Liang, P. Influences of pH value, temperature, chloride ions and sulfide ions on the corrosion behaviors of 316L stainless steel in the simulated cathodic environment of proton exchange membrane fuel cell. *J. Power Sources* **2014**, *272*, 448−456.
(109) Chebeir, M.; Liu, H. Oxidation of Cr (III)-Fe (III) mixed-phase hydroxides by chlorine: implications on the control of hexavalent chromium in drinking water. *Environ. Sci. Technol.* **2018**, *52* (14), 7663−7670.
(110) Volk, C.; Dundore, E.; Schiermann, J.; LeChevallier, M. Practical evaluation of iron corrosion control in a drinking water distribution system. *Water Res.* **2000**, *34* (6), 1967−1974.
(111) Matsch, S.; Böhni, H. Influence of temperature on the localized corrosion of stainless steels. *Russ. J. Electrochem.* **2000**, *36*, 1122−1128.

https://doi.org/10.1021/acsestengg.5c00260
ACS EST Engg. XXXX, XXX, XXX−XXX

(112) Park, J.; Matsch, S.; Böhni, H. Effects of temperature and chloride concentration on pit initiation and early pit growth of stainless steel. *J. Electrochem. Soc.* **2002**, *149* (2), B34.
(113) Carranza, R.; Alvarez, M. The effect of temperature on the passive film properties and pitting behaviour of a FeCrNi alloy. *Corros. Sci.* **1996**, *38* (6), 909−925.
(114) Hu, X.; Neville, A. The electrochemical response of stainless steels in liquid-solid impingement. *Wear* **2005**, *258* (1−4), 641−648.
(115) Li, L.; Wang, Z.; Zheng, Y. Interaction between pitting corrosion and critical flow velocity for erosion-corrosion of 304 stainless steel under jet slurry impingement. *Corros. Sci.* **2019**, *158*, 108084.
(116) Zheng, Z.; Zheng, Y. Erosion-enhanced corrosion of stainless steel and carbon steel measured electrochemically under liquid and slurry impingement. *Corros. Sci.* **2016**, *102*, 259−268.
(117) Wang, Z.; Zheng, Y.; Yi, J. The role of surface film on the critical flow velocity for erosion-corrosion of pure titanium. *Tribol. Int.* **2019**, *133*, 67−72.
(118) Du, Y.; Yang, G.; Chen, S.; Ren, Y. Research on the erosion-corrosion mechanism of 304 stainless steel pipeline of mine water in falling film flow. *Corros. Sci.* **2022**, *206*, 110531.
(119) Qu, S.; Duan, L.; Shi, Z.; Liang, X.; Lv, S.; Wang, G.; Liu, T.; Yu, R. Hydrochemical assessments and driving forces of groundwater quality and potential health risks of sulfate in a coalfield, northern Ordos Basin, China. *Sci. Total Environ.* **2022**, *835*, 155519.
(120) Gervais, M.; Dubuc, J.; Paquin, M.; Gonzalez-Merchan, C.; Genty, T.; Neculita, C. M. Comparative efficiency of three advanced oxidation processes for thiosalts oxidation in mine-impacted water. *Miner. Eng.* **2020**, *152*, 106349.
(121) Aoyama, T.; Sugawara, Y.; Muto, I.; Hara, N. In situ monitoring of crevice corrosion morphology of type 316L stainless steel and repassivation behavior induced by sulfate ions. *Corros. Sci.* **2017**, *127*, 131−140.
(122) Li, D.; Li, Z.; Yu, J.; Cao, N.; Liu, R.; Yang, M. Characterization of bacterial community structure in a drinking water distribution system during an occurrence of red water. *Appl. Environ. Microbiol.* **2010**, *76* (21), 7171−7180.
(123) Kuch, A. Investigations of the reduction and re-oxidation kinetics of iron (III) oxide scales formed in waters. *Corros. Sci.* **1988**, *28* (3), 221−231.
(124) Ryan, M. P.; Williams, D. E.; Chater, R. J.; Hutton, B. M.; McPhail, D. S. Why stainless steel corrodes. *Nature* **2002**, *415* (6873), 770−774.
(125) Wang, C.-L.; Guo, H.-D.; Fang, J.; Yu, S.-X.; Yue, X.-Q.; Hu, Q.-H.; Liu, C.-W.; Zhang, J.-X.; Zhang, R.; Xu, X.-S.; et al. The role of Cr content on the corrosion resistance of carbon steel and low-Cr steels in the CO2-saturated brine. *Pet. Sci.* **2023**, *20* (2), 1155−1168.
(126) Li, G.; Wu, W.; Chai, P.; Yang, X.; Song, L. Influence of Cr and Ni elements on the electrochemical and early corrosion behavior of FeMnAlC low-density steel. *J. Mater. Res. Technol.* **2023**, *23*, 5892−5906.
(127) Kim, J. K.; Kim, Y. H.; Lee, J. S.; Kim, K. Y. Effect of chromium content on intergranular corrosion and precipitation of Ti-stabilized ferritic stainless steels. *Corros. Sci.* **2010**, *52* (5), 1847−1852.
(128) Korzhavyi, P. A.; Sandström, R. First-principles evaluation of the effect of alloying elements on the lattice parameter of a 23Cr25NiWCuCo austenitic stainless steel to model solid solution hardening contribution to the creep strength. *Mater. Sci. Eng., A* **2015**, *626*, 213−219.
(129) Zhang, M.; Kim, K. H.; Shao, Z.; Wang, F.; Zhao, S.; Suo, N. Effects of Mo content on microstructure and corrosion resistance of arc ion plated Ti-Mo-N films on 316L stainless steel as bipolar plates for polymer exchange membrane fuel cells. *J. Power Sources* **2014**, *253*, 201−204.
(130) Heuer, A.; Ernst, F.; Kahn, H.; Avishai, A.; Michal, G.; Pitchure, D.; Ricker, R. Interstitial defects in 316L austenitic stainless steel containing "colossal" carbon concentrations: An internal friction study. *Scr. Mater.* **2007**, *56* (12), 1067−1070.
(131) Williamson, D.; Li, W.; Wei, R.; Wilbur, P. Solid solution strengthening of stainless steel surface layers by rapid, high-dose, elevated temperature nitrogen ion implantation. *Mater. Lett.* **1990**, *9* (9), 302−308.
(132) Lai, J. K. L.; Shek, C. H.; Lo, K. H. *Stainless Steels: An Introduction and Their Recent Developments*; Bentham Science Publishers, 2012.
(133) Abreu, C.; Cristóbal, M.; Losada, R.; Nóvoa, X.; Pena, G.; Pérez, M. The effect of Ni in the electrochemical properties of oxide layers grown on stainless steels. *Electrochim. Acta* **2006**, *51* (15), 2991−3000.
(134) Wang, Z.; Feng, Z.; Zhang, L. Effect of high temperature on the corrosion behavior and passive film composition of 316 L stainless steel in high H2S-containing environments. *Corros. Sci.* **2020**, *174*, 108844.
(135) Baba, H.; Kodama, T.; Katada, Y. Role of nitrogen on the corrosion behavior of austenitic stainless steels. *Corros. Sci.* **2002**, *44* (10), 2393−2407.
(136) Bayoumi, F. M.; Ghanem, W. A. Effect of nitrogen on the corrosion behavior of austenitic stainless steel in chloride solutions. *Mater. Lett.* **2005**, *59* (26), 3311−3314.
(137) Pardo, A.; Merino, M.; Coy, A.; Viejo, F.; Arrabal, R.; Matykina, E. Effect of Mo and Mn additions on the corrosion behaviour of AISI 304 and 316 stainless steels in H2SO4. *Corros. Sci.* **2008**, *50* (3), 780−794.
(138) Lynch, B.; Wang, Z.; Ma, L.; Paschalidou, E.-M.; Wiame, F.; Maurice, V.; Marcus, P. Passivation-induced Cr and Mo enrichments of 316L stainless steel surfaces and effects of controlled pre-oxidation. *J. Electrochem. Soc.* **2020**, *167* (14), 141509.
(139) Dong, Z.; Li, M.; Behnamian, Y.; Luo, J.-L.; Chen, W.; Amirkhiz, B. S.; Liu, P.; Pang, X.; Li, J.; Zheng, W.; et al. Effects of Si, Mn on the corrosion behavior of ferritic-martensitic steels in supercritical water (SCW) environments. *Corros. Sci.* **2020**, *166*, 108432.
(140) Torres, C.; Johnsen, R.; Iannuzzi, M. Crevice corrosion of solution annealed 25Cr duplex stainless steels: effect of W on critical temperatures. *Corros. Sci.* **2021**, *178*, 109053.
(141) Jeon, S.-H.; Kim, S.-T.; Lee, I.-S.; Kim, J.-S.; Kim, K.-T.; Park, Y.-S. Effects of W substitution on the precipitation of secondary phases and the associated pitting corrosion in hyper duplex stainless steels. *J. Alloys Compd.* **2012**, *544*, 166−172.
(142) Dossett, J. L.; Totten, G. E. *Heat Treating of Irons and Steels*; ASM international, 2014.
(143) Yu, X.; Chen, S.; Wang, L. Effect of solution treatment conditions on the sensitization of austenitic stainless steel. *J. Serb. Chem. Soc.* **2009**, *74* (11), 1293−1302.
(144) Sourisseau, T.; Chauveau, E.; Baroux, B. Mechanism of copper action on pitting phenomena observed on stainless steels in chloride media. *Corros. Sci.* **2005**, *47* (5), 1097−1117.
(145) Banas, J.; Mazurkiewicz, A. The effect of copper on passivity and corrosion behaviour of ferritic and ferritic-austenitic stainless steels. *Mater. Sci. Eng., A* **2000**, *277* (1−2), 183−191.
(146) Wang, X.; Shen, X. Research Progress of ODS FeCrAl Alloys-A Review of Composition Design. *Materials* **2023**, *16* (18), 6280.
(147) Zhang, W.; Liu, F.; Liu, L.; Li, Q.; Liu, L.; Liu, F.; Huang, C. Effect of grain size and distribution on the corrosion behavior of Y_2O_3 dispersion-strengthened 304 stainless steel. *Mater. Today Commun.* **2022**, *31*, 103723.
(148) Guo, X.; Chen, K.; Gao, W.; Shen, Z.; Zhang, L. Corrosion behavior of alumina-forming and oxide dispersion strengthened austenitic 316 stainless steel in supercritical water. *Corros. Sci.* **2018**, *138*, 297−306.
(149) Zhao, H.; Liu, T.; Bai, Z.; Wang, L.; Gao, W.; Zhang, L. Corrosion behavior of 14Cr ODS steel in supercritical water: The influence of substituting Y_2O_3 with $Y_2Ti_2O_7$ nanoparticles. *Corros. Sci.* **2020**, *163*, 108272.
(150) Bischoff, J.; Motta, A. T. Oxidation behavior of ferritic-martensitic and ODS steels in supercritical water. *J. Nucl. Mater.* **2012**, *424* (1−3), 261−276.

https://doi.org/10.1021/acsestengg.5c00260
ACS EST Engg. XXXX, XXX, XXX−XXX

(151) Miao, Y.; Mo, K.; Zhou, Z.; Liu, X.; Lan, K.-C.; Zhang, G.; Miller, M. K.; Powers, K. A.; Almer, J.; Stubbins, J. F. In situ synchrotron tensile investigations on the phase responses within an oxide dispersion-strengthened (ODS) 304 steel. *Mater. Sci. Eng., A* **2015**, *625*, 146−152.
(152) Guo, X.; Chen, K.; Gao, W.; Shen, Z.; Lai, P.; Zhang, L. A research on the corrosion and stress corrosion cracking susceptibility of 316L stainless steel exposed to supercritical water. *Corros. Sci.* **2017**, *127*, 157−167.
(153) Li, L.-F.; Caenen, P.; Daerden, M.; Vaes, D.; Meers, G.; Dhondt, C.; Celis, J.-P. Mechanism of single and multiple step pickling of 304 stainless steel in acid electrolytes. *Corros. Sci.* **2005**, *47* (5), 1307−1324.
(154) O'Laoire, C.; Timmins, B.; Kremer, L.; Holmes, J.; Morris, M. Analysis of the acid passivation of stainless steel. *Anal. Lett.* **2006**, *39* (11), 2255−2271.
(155) Geng, S.; Sun, J.; Guo, L. Effect of sandblasting and subsequent acid pickling and passivation on the microstructure and corrosion behavior of 316L stainless steel. *Mater. Des.* **2015**, *88*, 1−7.
(156) Maller, R. R. Passivation of stainless steel. *Trends Food Sci. Technol.* **1998**, *9* (1), 28−32.
(157) Penttilä, S.; Toivonen, A.; Li, J.; Zheng, W.; Novotny, R. Effect of surface modification on the corrosion resistance of austenitic stainless steel 316L in supercritical water conditions. *J. Supercrit. Fluids* **2013**, *81*, 157−163.
(158) de Oliveira, A. C.; de Oliveira, M. L.; Ríos, C.; Antunes, R. The effect of mechanical polishing and finishing on the corrosion resistance of AISI 304 stainless steel. *Corros. Eng. Sci. Technol.* **2016**, *51* (6), 416−428.
(159) Łyczkowska-Widłak, E.; Lochyński, P.; Nawrat, G. Electrochemical polishing of austenitic stainless steels. *Materials* **2020**, *13* (11), 2557.
(160) Mai, T.; Lim, G. Micromelting and its effects on surface topography and properties in laser polishing of stainless steel. *J. Laser Appl.* **2004**, *16* (4), 221−228.
(161) Betts, A.; Boulton, L. Crevice corrosion: review of mechanisms, modelling, and mitigation. *Br. Corros. J.* **1993**, *28* (4), 279−296.
(162) Fu, J.; Li, F.; Sun, J.; Wu, Y. Texture, orientation, and mechanical properties of Ti-stabilized Fe-17Cr ferritic stainless steel. *Mater. Sci. Eng., A* **2018**, *738*, 335−343.
(163) Żuk, M.; Czupryński, A.; Czarnecki, D.; Poloczek, T. The effect of niobium and titanium in base metal and filler metal on intergranular corrosion of stainless steels. *Weld. Technol. Rev.* **2019**, *91* (6), 30−38.
(164) Bekmurzayeva, A.; Duncanson, W. J.; Azevedo, H. S.; Kanayeva, D. Surface modification of stainless steel for biomedical applications: Revisiting a century-old material. *Mater. Sci. Eng., C* **2018**, *93*, 1073−1089.
(165) Ye, C.; Zhu, Y.; Sun, H.; Chen, F.; Sun, H.; Dai, W.; Wei, Q.; Fu, L.; Yu, A.; Du, S.; et al. Layer-by-layer stacked graphene nanocoatings by Marangoni self-assembly for corrosion protection of stainless steel. *Chin. Chem. Lett.* **2021**, *32* (1), 501−505.
(166) Ibrahim, M.; Korablov, S.; Yoshimura, M. Corrosion of stainless steel coated with TiN, (TiAl)N and CrN in aqueous environments. *Corros. Sci.* **2002**, *44* (4), 815−828.
(167) Krishna, N.; Thinaharan, C.; George, R.; Parvathavarthini, N.; Kamachi Mudali, U. Surface modification of type 304 stainless steel with duplex coatings for corrosion resistance in sea water environments. *Surf. Eng.* **2015**, *31* (1), 39−47.
(168) Dai, J.; Yang, J.; Zhuge, L.; Wu, X. Al2O3-TiO2 composite coatings with enhanced anticorrosion properties for 316L stainless steel. *Mater. Corros.* **2020**, *71* (9), 1512−1520.
(169) Zhang, X.-F.; Chen, Y.-Q.; Hu, J.-M. Robust superhydrophobic SiO2/polydimethylsiloxane films coated on mild steel for corrosion protection. *Corros. Sci.* **2020**, *166*, 108452.
(170) Padhy, N.; Kamal, S.; Chandra, R.; Mudali, U. K.; Raj, B. Corrosion performance of TiO_2 coated type 304L stainless steel in nitric acid medium. *Surf. Coat. Technol.* **2010**, *204* (16−17), 2782−2788.
(171) Li, L.; Yan, J.; Xiao, J.; Sun, L.; Fan, H.; Wang, J. A comparative study of corrosion behavior of S-phase with AISI 304 austenitic stainless steel in $H_2S/CO_2/Cl^-$ media. *Corros. Sci.* **2021**, *187*, 109472.
(172) Liao, J.; Kishimoto, K.; Yao, M.; Mori, Y.; Ikai, M. Effect of ozone on corrosion behavior of mild steel in seawater. *Corros. Sci.* **2012**, *55*, 205−212.
(173) Wang, H.; Hu, C.; Zhang, S.; Liu, L.; Xing, X. Effects of O3/Cl2 disinfection on corrosion and opportunistic pathogens growth in drinking water distribution systems. *J. Environ. Sci.* **2018**, *73*, 38−46.
(174) Cao, K. F.; Chen, Z.; Shi, Q.; Wu, Y. H.; Lu, Y.; Mao, Y.; Chen, X. W.; Li, K.; Xu, Q.; Hu, H. Y. An insight to sequential ozone-chlorine process for synergistic disinfection on reclaimed water: Experimental and modelling studies. *Sci. Total Environ.* **2021**, *793*, 148563.
(175) Seridou, P.; Kalogerakis, N. Disinfection applications of ozone micro-and nanobubbles. *Environ. Sci.: Nano* **2021**, *8* (12), 3493−3510.
(176) Fernando, W. A. M.; Ilankoon, I.; Syed, T. H.; Yellishetty, M. Challenges and opportunities in the removal of sulphate ions in contaminated mine water: A review. *Miner. Eng.* **2018**, *117*, 74−90.
(177) Tan, C.; Liu, H. Inhibition of Hexavalent Chromium Release from Drinking Water Distribution Systems: Effects of Water Chemistry-Based Corrosion Control Strategies. *Environ. Sci. Technol.* **2023**, *57* (47), 18433−18442.
(178) Askari, F.; Ghasemi, E.; Ramezanzadeh, B.; Mahdavian, M. Mechanistic approach for evaluation of the corrosion inhibition of potassium zinc phosphate pigment on the steel surface: application of surface analysis and electrochemical techniques. *Dyes Pigm.* **2014**, *109*, 189−199.
(179) Tanane, O.; Abboud, Y.; Aitenneite, H.; El Bouari, A. Corrosion inhibition of the 316L stainless steel in sodium hypochlorite media by sodium silicate. *J. Mater. Environ. Sci.* **2016**, *7* (1), 131−138.
(180) Orlikowski, J.; Darowicki, K.; Jazdzewska, A.; Jarzynka, M. The protection and monitoring of a distribution piping network for potable water supply. *Anti-Corros. Methods Mater.* **2015**, *62* (6), 400−406.
(181) Maddison, L. A.; Gagnon, G. A.; Eisnor, J. D. Corrosion control strategies for the Halifax regional distribution system. *Can. J. Civ. Eng.* **2001**, *28* (2), 305−313.
(182) Cantor, A. F.; Park, J. K.; Vaiyavatjamai, P. Effect of chlorine on corrosion in drinking water systems. *J. Am. Water Works Assn.* **2003**, *95* (5), 112−123.
(183) Al-Amiery, A. A.; Yousif, E.; Isahak, W. N. R. W.; Al-Azzawi, W. K. A review of inorganic corrosion inhibitors: types, mechanisms, and applications. *Tribol. Ind.* **2023**, *44* (2), 313.
(184) De Ketelaere, E.; Moed, D.; Vanoppen, M.; Verliefde, A.; Verbeken, K.; Depover, T. Sodium silicate corrosion inhibition behaviour for carbon steel in a dynamic salt water environment. *Corros. Sci.* **2023**, *217*, 111119.
(185) Tian, Y.; Zheng, M. Inhibition effect of silicate and molybdate on the corrosion of SS 316 in neutral corrosive solution at high temperature. *Mater. Res. Express* **2019**, *6* (9), 096569.
(186) Nkhoma, R. K.; Siyasiya, C. W.; Stumpf, W. E. Hot workability of AISI 321 and AISI 304 austenitic stainless steels. *J. Alloys Compd.* **2014**, *595*, 103−112.
(187) Ma, X.; Wang, L.; Liu, C.; Subramanian, S. Microstructure and properties of 13Cr5Ni1Mo0. 025Nb0. 09V0. 06N super martensitic stainless steel. *Mater. Sci. Eng., A* **2012**, *539*, 271−279.
(188) Chen, T.; Weng, K.; Yang, J. The effect of high-temperature exposure on the microstructural stability and toughness property in a 2205 duplex stainless steel. *Mater. Sci. Eng., A* **2002**, *338* (1−2), 259−270.
(189) Alizadeh-Sh, M.; Marashi, S.; Pouranvari, M. Resistance spot welding of AISI 430 ferritic stainless steel: phase transformations and mechanical properties. *Mater. Des.* **2014**, *56*, 258−263.

https://doi.org/10.1021/acsestengg.5c00260
ACS EST Engg. XXXX, XXX, XXX−XXX